Water Resources Research

RESEARCH ARTICLE
10.1029/2021WR031275

Catchment Dissolved Organic Carbon Transport: A Modeling Approach Combining Water Travel Times and Reactivity Continuum

G. Grandi[1] **and E. Bertuzzo**[1]

[1]Department of Environmental Sciences, Informatics and Statistics, University of Venice Ca' Foscari, Venice, Italy

Key Points:

- Quantity and reactivity of dissolved organic carbon (DOC) exported from a hillslope are modeled coupling water age and reactivity continuum
- The age structure of water in the catchment controls DOC degradation within soils
- DOC concentration-discharge relations are explained by water travel time distribution

Supporting Information:

Supporting Information may be found in the online version of this article.

Correspondence to:

E. Bertuzzo,
enrico.bertuzzo@unive.it

Citation:

Grandi, G., & Bertuzzo, E. (2022). Catchment dissolved organic carbon transport: A modeling approach combining water travel times and reactivity continuum. *Water Resources Research*, *58*, e2021WR031275. https://doi.org/10.1029/2021WR031275

Received 23 SEP 2021
Accepted 29 JUN 2022

Author Contributions:

Conceptualization: G. Grandi, E. Bertuzzo
Data curation: G. Grandi
Investigation: G. Grandi
Methodology: G. Grandi, E. Bertuzzo
Supervision: E. Bertuzzo
Writing – original draft: G. Grandi, E. Bertuzzo
Writing – review & editing: G. Grandi, E. Bertuzzo

Abstract Quantifying the transfer of organic carbon from the terrestrial to the riverine ecosystems is of crucial importance to fully appreciate the carbon cycle at the catchment, regional and global scales. In this study, we propose a framework for modeling the flux of dissolved organic carbon (DOC) from hillslopes to stream and river networks which couples a transport model based on travel time distributions with the reactivity continuum (RC) approach to model DOC degradation. We test the model by applying it to the Plynlimon catchments (UK) exploiting both weekly and high-frequency (7-hr interval) time-series. We use information about chloride to get an independent estimate of water travel times using the framework of StorAge Selection functions. Following the RC model, the composition and the degradation of DOC along the flowpaths, and its consequent concentration in the streamflow, is described assuming that DOC is composed by a mixture of compounds that follows a continuous spectrum of reactivity. For the high-frequency data set, the model is able to reproduce DOC streamflow concentrations and to capture the complex hysteretic relation between DOC concentration and discharge. Weekly data are instead not frequent enough to properly describe DOC dynamics in this catchment. The distribution of the age of the water comprised in the streamflow proves thus a key variable to predict the quantity and the reactivity of the DOC exported from soils, and the effect of hydrologic variability on this process.

Plain Language Summary Streams and rivers are able to drain, transport, process and mineralize the carbon stored in the terrestrial ecosystems. This set of processes controls stream water quality, the metabolic functioning of riverine ecosystems, and eventually the carbon balance and the CO_2 emissions at the global scale. We focus on the flux of dissolved organic carbon (DOC) originating from the decomposition of soil organic matter and exported from hillslopes to the streamflow by rainfall-runoff processes. Our goal is to contribute to the understanding of this process and to disentangle the complex relation between DOC concentration and discharge. We estimate the quantity of DOC that survives the pathways from the soil to the stream using two key variables: the time that the water transporting DOC spends along the pathway and the DOC reactivity, which controls its degradation. The model is able to capture the complex behavior of stream DOC concentration in two headwater catchments, suggesting that the mixture of water with different ages that characterizes the streamflow controls the time available for degradation and thus the flux of DOC exported.

1. Introduction

Streams and rivers are important contributors to the global carbon cycle despite the limited area they cover on the Earth's surface (Cole et al., 2007; Battin et al., 2008, 2009). They connect the terrestrial to the marine ecosystems and function as biogeochemical reactors able to collect, transport and process carbon. Current estimates of CO_2 released by freshwater suggest that they are of the same magnitude as the net ocean-atmosphere exchange, albeit in the opposite direction (Aufdenkampe et al., 2011; Battin et al., 2009; Raymond et al., 2013; Tranvik et al., 2009). Despite the numerous evidence collected, the magnitude of these fluxes is still poorly constrained and may be underestimated (Drake et al., 2018). This paper focuses on the export of organic carbon, and in particular DOC, from land into streams within the hydrologic cycle. Understanding the entity of DOC fluctuations in streamflow is of crucial interest for quantifying their impact not only on CO_2 global balance, but also on the fluvial metabolic balance and nutrient cycles, and eventually on water quality, with implications also for drinking water treatment (Evans et al., 2005; Ritson et al., 2014).

Within the critical zone, organic matter from the terrestrial ecosystem is continuously transformed and processed mainly by microorganisms (Lehmann & Kleber, 2015). Among the different states and forms in which carbon is

present in the soil, DOC is a critical intermediate step in the degradation and transformation processes. Within this very reactive soil-atmosphere-water interface, carbon and water cycles are tightly connected (Manzoni et al., 2012; Moyano et al., 2013). Moreover, during streamflow producing events (precipitation or snowmelt), DOC is exported from soil to streams along with the flow (Raymond & Saiers, 2010), with the majority of the mass typically exported during few intense precipitation and flow events (Raymond et al., 2016). Several studies have investigated the relation between DOC concentration and discharge disclosing a hysteretic behavior (Boyer et al., 1997; Butturini et al., 2006; Hornberger et al., 1994; Tunaley et al., 2016), especially during high discharge events when DOC concentration can vary considerably (Raymond & Saiers, 2010; Saraceno et al., 2009; Sawyer et al., 2014). Hydrology plays thus a primary role in controlling DOC dynamics but other long-term drivers for the variation of DOC concentration in the streamflow have been identified in land-use, temperature, climate, seasonality (Butturini & Sabater, 2000; Clark et al., 2010; Evans et al., 2005; Manzoni et al., 2012; Raymond & Saiers, 2010; Regier et al., 2016; Saraceno et al., 2009) and landscape heterogeneity (Catalán et al., 2013; Ågren et al., 2014).

Focusing on a single event, the concentration of DOC measured during the rising phase of the hydrograph is typically higher than the one observed during the falling phase for the same value of discharge (Fasching et al., 2016; Raymond & Saiers, 2010). This hysteretic behavior has been attributed to the evolving contribution of different hydrologic pathways to streamflow during the different phases of the hydrograph (Raymond & Saiers, 2010). During intense rainfall events, the rising part of the hydrograph can be dominated by short flow pathways that interact mostly with carbon-rich superficial soil layers and thus result in high DOC export. During the falling phase of the hydrograph instead, slower pathways (e.g., subsuperficial and groundwater components) characterized by lower DOC concentration (as most of the labile DOC has already been degraded) become more relevant (see Raymond and Saiers (2010) and references therein). The travel time of water within the soil (defined as the time elapsed from its entrance as precipitation and its exit as discharge) and the reactivity (i.e., lability) of the DOC transported along are thus suggested to be two crucial drivers of the concentration and composition of DOC exported from soil to streams. The former dictates the time available for degradation, while the latter the rate of such process. The relation between water travel time and export of DOC has already been addressed in the literature (e.g., Barua et al., 2022; Dawson et al., 2008; Lyon et al., 2010; Tiwari et al., 2014). Building on this previous applications, we propose a model that improves the description of travel time and DOC cycling. Specifically, we develop a framework that couples two emerging probabilistic approaches to model (a) time-variant travel time distributions (TTDs) in the hydrological cycle and (b) the degradation of DOC accounting for a continuous description of its reactivity.

The hydrological community has long wondered how much time water spends within hillslopes, catchments or aquifers (e.g., Haggerty et al., 2002; Jury et al., 1986; Kreft & Zuber, 1978; Maloszewski et al., 1992). Indeed, understanding how hydrological systems retain and release water can shed light on underlying hydrological processes, flowpath connectivity and ultimately on water quality. The travel time of water within a hydrological system is usually assumed to be a random variable due to the inherent complexity and variability of such systems, and therefore it is typically described through the related probability distribution. To consistently define catchment-scale TTDs that vary in time due to hydrological fluctuations, a new approach has gained momentum (Botter et al., 2010, 2011; Rinaldo et al., 2011, 2015; Hrachowitz et al., 2013; van der Velde et al., 2014; Harman, 2015; Kirchner, 2015a, 2015b). Such approach specifies, through suitable StorAge Selection functions (SAS) (Rinaldo et al., 2015) how outgoing fluxes (say, discharge or evapotranspiration) draw from the available ages of water particles stored in the hydrological system. A large array of applications now features time-variant TTDs and sampling functions (see e.g., Benettin, Bailey, et al., 2015; Benettin, Rinaldo, et al., 2015; Bertuzzo et al., 2013; Birkel et al., 2012; Harman, 2015; Harman & Kim, 2014; Heidbüchel et al., 2012; Hrachowitz et al., 2013; McMillan et al., 2012; Rigon et al., 2016; Soulsby et al., 2015; van der Velde et al., 2010).

Most soil carbon cycling models considers a complex system of active pools through which carbon inputs from litterfall are processed by microbial activity (Jenkinson & Coleman, 2008; Jenkinson et al., 1990, 2008; Nakhavali et al., 2018; Parton et al., 1987, 1993; Swift et al., 1979). According to this representation, organic carbon is thus available under different qualities, from labile to recalcitrant or inert, depending on the degradation processes it has been involved. Fresh biomass in input from the terrestrial ecosystem is processed into DOC by means of bacterial metabolism and thus gradually decomposed, resulting in a loss of carbon via respiration (i.e., CO_2) and in a change in quality toward more recalcitrant components. The process of decomposition consists

thus in the elaboration of the highly degradable (i.e., labile) molecules of DOC and in the consequent release of more stable (i.e., recalcitrant) ones. This heterogeneity has often been represented as a system of discrete carbon pools through which degradation occurs in series or in parallel steps, each one typically characterized by a linear (less frequently, nonlinear) degradation kinetics (Manzoni & Porporato, 2009). Noticeably, these models can be very complex when they consider a large number of fluxes, the presence of feedback, temperature influence and diffusion between different soil layers. The clear disadvantage in using these multi-compartment models is the large number of parameters required for their description. In order to reduce such complexity, a continuum quality theory has been proposed (Bosatta & Ågren, 1985, 2003; Carpenter, 1981; Nilsson et al., 2005). Continuous models consider that carbon mass can flow from a quality to another through a continuous spectrum, using a continuous quality index instead of a discrete number of pools (Bosatta & Ågren, 1996). Here, we use the particular case of the RC model (Bosatta & Ågren, 1995b; Boudreau & Ruddick, 1991) to describe DOC decomposition. This model, which can be thought of as a particular case of the more general q-theory (Bosatta & Ågren, 1995b), characterizes carbon quality through its corresponding reactivity, that is, its first order decay rate, and describes the distribution of carbon density among the continuous spectrum of reactivity through a suitable probability density function. We thus integrate the SAS framework with the RC model in order to jointly estimate the TTDs of water parcels in streamflow and the quantity and reactivity of DOC they export. Specifically, the model accounts for the mass density of DOC of a certain age (i.e., the age of the water carrying it) and reactivity in the export flux at a certain time. We apply the model using data collected at the Plynlimon research catchments (Neal et al., 2010, 2012). As different combinations of water age mixture and degradation rate can lead to similar DOC concentration observed in the streamflow, in addition to DOC data, we use also information about chloride (treated as a non reactive solute) to gain independent knowledge about TTDs.

The paper is organized as follows: Section 2 develops the general framework that combines the SAS and the RC model approaches. The description of the site and details about the model formulation are described in Section 3. Results are presented in Section 4 and discussed in Section 5. A set of conclusions (Section 6) closes the paper.

2. Theoretical Framework

2.1. Water Age

A comprehensive account of time-variant TTDs approaches and sampling functions is reported elsewhere (Botter et al., 2011; Harman, 2015; Rinaldo et al., 2015; Sprenger et al., 2019; van der Velde et al., 2014). However, for the paper to be self-contained, this section illustrates the main concepts and definitions. Let us consider a hydrologic control volume with a storage $S(t)$ of water which changes in time as a result of intermittent input $J(t)$ (e.g., precipitation) and a time-variable output flux $Q(t)$ (e.g., discharge). For the sake of simplicity we illustrate the framework with a single output flux, but the model can be readily generalized to account for multiple output fluxes (say to model evapotranspiration, see e.g., Botter et al., 2011; Harman, 2015; Benettin, Rinaldo, et al., 2015). The age or residence time T of a drop of water stored within the control volume is defined as the time elapsed since its entrance as J. Accordingly, the age structure of the volume $S(t)$ can be described by the residence time distribution (RTD) $p_S(T,t)$ – the probability density function of the residence time of all water particles stored within the control volume at time t. The residence time that a water drop has when leaving the system as Q is termed travel time. The corresponding TTD, $p_Q(T,t)$ (Benettin, Rinaldo, et al., 2015; Cvetkovic et al., 2012; Niemi, 1977; Rinaldo et al., 2011), refers to the set of particles that are simultaneously leaving the system as Q at time t and measures the time elapsed since their entrance. Formally, this distribution is referred to as backward TTD to differentiate it from the forward one (for a detailed treatment, the reader is referred to Benettin, Rinaldo, et al., 2015). In the following we will solely refer to the backward TTD as it is suitable to characterize the age composition of a sample of stream water. The intertwined relation between RTD and TTD is readily evident by focusing on the time evolution of the quantity $s(T,t)dT = S(t)p_S(T,t)dT$: the infinitesimal volume of water with residence time around T contained within the system at time t, which obeys to the following partial differential equation:

$$\frac{\partial s(T,t)}{\partial t} + \frac{\partial s(T,t)}{\partial T} = -Q(t)p_Q(T,t), \tag{1}$$

with boundary conditions $s(0,t) = J(t)$. In Equation 1, the variation in time of $s(T,t)$ is expressed in terms of aging (second term of the left-hand side) and removal by Q (right-hand side). It is convenient (Harman, 2015; Rinaldo et al., 2015; van der Velde et al., 2014) to express Equation 1 in an integral form as:

$$\frac{\partial S_T(T,t)}{\partial t} + \frac{\partial S_T(T,t)}{\partial T} = -Q(t)P_Q(T,t) + J(t), \tag{2}$$

where the variable $S_T(T,t)$ represents the rank storage: the storage younger than T at a given time t, and it is defined as:

$$S_T(T,t) = \int_0^T s(\tau,t)d\tau = S(t)\int_0^T p_S(\tau,t)d\tau = S(t)P_S(T,t). \tag{3}$$

In Equation 3, $P_S(T,t)$ represents the cumulative distribution of $p_S(T,t)$, that is, the fraction of water in storage that is younger than T at a given time t. Analogously, $P_Q(T,t)$ is the cumulative distribution of $p_Q(T,t)$.

The closure of the problem requires the specification of how outgoing fluxes sample the available ages in storage, that is, the relation between $P_Q(T,t)$ and $P_S(T,t)$. To that end we exploit the formulation of the problem through SAS functions (Harman, 2015; Rinaldo et al., 2015; van der Velde et al., 2014). Specifically, we use SAS functions expressed in terms of cumulative distribution functions of the rank storage S_T. The discharge SAS function $\Omega_Q(S_T(T,t),t)$ is defined as the fraction of discharge that is contributed by $S_T(T,t)$, the water in storage younger than T. By definition, one thus has that $\Omega_Q(S_T(T,t),t) = P_Q(T,t)$. Combing the latter with Equation 1 allows solving for $P_S(T,t)$.

The concentration $C_Q(t)$ in the outflow discharge of a conservative tracer that enters the control volume through input $J(t)$ can be expressed as:

$$C_Q(t) = \int_0^\infty dT\, C_J(t-T)p_Q(T,t), \tag{4}$$

that is, as a weighted sum of previous input concentrations $C_J(t-T)$, where the weight is provided by the contribution of water of age T in the discharge at time t, that is, the backward TTDs $p_Q(T,t)$.

2.2. Reactivity Continuum

The continuous quality theory (q-theory) assumes that carbon mass can be represented according to a certain distribution of lability defined using a continuous quality index $I(q)$ (Ågren & Bosatta, 1996; Aris, 1989; Bosatta & Ågren, 1985, 1991a, 1991b, 1994, 1995a; Boudreau & Ruddick, 1991; Carpenter, 1981, 1982; Tarutis, 1994) instead of a series of dicrete compartments. Introducing the mass density $\rho(q,t)$ (where $\rho(q,t)dq$ represents the infinitesimal mass of quality around q at time t), the total mass can be expressed as:

$$M(t) = \int_0^\infty \rho(q,t)dq. \tag{5}$$

Index $I(q)$ represents DOC accessibility to degradation: labile DOC parcels are expected to be elaborated rapidly while more recalcitrant parcels have a lower degradation rate (Bosatta & Ågren, 1991a). Each element can flow from a quality (q) to a more recalcitrant one (q') when submitted to decomposition process following a transition probability density distribution ($D(q,q')$) (Ågren & Bosatta, 1996; Bosatta & Ågren, 2003; Manzoni et al., 2009). Assuming the simplest form for $D(q,q')$, which is the case of the Dirac δ-distribution ($D(q,q') = \delta(q-q')$), that is, assuming that during the degradation step no change in quality is observed, the problem reduces to the particular case of the RC model and it represents the continuum description of a set of linear compartments in parallel (Aris, 1989; Bosatta & Ågren, 1995b; Boudreau & Ruddick, 1991; Burnham & Braun, 1999; Manzoni et al., 2009). A reasonable choice is to assume as quality index the reactivity, that is, the corresponding first order decay rate ($I(q) = k(q)$), associated to the quality q, so that the total DOC mass is composed by a distribution of parcels characterized by different reactivity. Considering that each component decays following a first order kinetic, the time evolution of the density $\rho(q,t)$ obeys the following ordinary differential equation:

$$\frac{d\rho(q,t)}{dt} = -k(q)\rho(q,t), \tag{6}$$

where the initial condition $\rho(q,0)$ represents the initial distribution of reactivity. The solution of Equation 6 can straightforwardly be derived as $\rho(q,t) = \rho(q,0)e^{-k(q)t}$. The number of parameters required for the definition of the model depends on the form assumed for $\rho(q,0)$ (e.g., gamma, beta, or lognormal distributions) but it is usually parsimonious with respect to models with discrete compartments (Aris, 1965; Boudreau & Ruddick, 1991; Manzoni et al., 2009; Vähätalo et al., 2010).

2.3. Coupling Water Age and Reactivity Continuum Models

The aim of the model presented herein is hence to integrate the two previous approaches in order to estimate the flux of DOC transferred from the soil to the streamflow. The system is described by the density $\rho(q,T,t)$ contained in the control volume. Specifically $\rho(q,T,t)dq\,dT$ represents the mass of DOC of reactivity around q transported by water parcels with a residence time around T at time t. Along with $\rho(q,T,t)$, it is analogously possible to define the concentration reactivity distribution $C(q,T,t)$ (i.e., the mass density per unit volume) as $\rho(q,T,t)/s(T,t)$. We assume that water parcels, after passing through the carbon rich soil top layer, carry an initial DOC concentration. Such concentration can vary in time to account for seasonal variations in soil organic carbon content and microbial activity that can favor its dissolution into DOC. We term $C_0(q,t)$ the reactivity distribution of the initial DOC concentration. Along the flowpath, DOC undergoes degradation according to the RC model whereas the time available for degradation is controlled by the travel time of water parcels. The governing equation for $\rho(q,T,t)$ can be obtained combining Equations 1 and 6:

$$\frac{\partial \rho(q,T,t)}{\partial t} + \frac{\partial \rho(q,T,t)}{\partial T} = -k(q)\rho(q,T,t) - \frac{p_Q(T,t)Q(t)}{s(T,t)}\rho(q,T,t). \tag{7}$$

with boundary conditions $\rho(q,T=0,t) = C_0(q,t)J(t)$. Equation 7 describes density variation in terms of aging (second term of the left hand side), degradation (first term of the right hand side) and export (second term of the right hand side). The concentration of DOC in the discharge Q can be obtained integrating the last term of Equation 7 over q and T (i.e., to obtain the total mass flux of exported DOC) and dividing by the discharge $Q(t)$.

$$\begin{aligned} C_Q(t) = \int_0^\infty dT\, p_Q(T,t) \int_0^\infty dq\, \frac{\rho(q,T,t)}{s(T,t)} = \\ \int_0^\infty dT\, p_Q(T,t) \int_0^\infty dq\, C(q,T,t) = \int_0^\infty dT\, p_Q(T,t) C(T,t), \end{aligned} \tag{8}$$

where $C(T,t)$ represents the DOC concentration in water parcels of age T at time t. The right hand side of Equation 8 highlights the analogy to the case of conservative solutes (Equation 4). The concentration of a conservative solute does not change along the flowpath, and thus it remains equal to that of the input: $C(T,t) = C_J(t-T)$. In the case of a reactive solute like DOC, $C(T,t)$ must be explicitly evaluated solving the coupled system of Equations 1 and 7.

3. Model Application

3.1. Site and Data

We applied the model to the Hafren stream comprised within the Plynlimon experimental catchments (Wales) (Figure 1), for which the UK Centre of Ecology and Hydrology (CEH) provides two extensive hydrological and geochemical data sets: one long-term record (around 25 years) sampled at roughly weekly intervals, and a shorter one (1.5 years) sampled every 7 hr (https://gateway.ceh.ac.uk/). We modeled streamflow concentration of both chloride (treated as a conservative tracer) and DOC. As the two solutes show markedly different temporal dynamics (Figures 2 and 3), we were interested in understanding the effects of both sampling frequency and duration of the observation period on parameter estimation. We thus applied the model using both datasets: at weekly frequency in the Lower Hafren (catchment area 3.58 km^2) and at high-frequency in the Upper Hafren (a subcatchment of 1.22 km^2). This choice ensured the use of the most complete data series in both cases. A detailed meteorological and environmental description of these experimental catchments can be found extensively in literature (Haria & Shand, 2004; Kirby et al., 1991; Kirchner, 2009; Kirchner et al., 2000; Knapp et al., 2019; Lee et al., 2020; Neal et al., 1990, 2001, 2010, 2012, 2013; Neal & Kirchner, 2000; Neal, Robson, et al., 1997; Neal, Wilkinson, et al., 1997; Page et al., 2007; Remondi et al., 2018). Here, we briefly summarize the features of interest for our application.

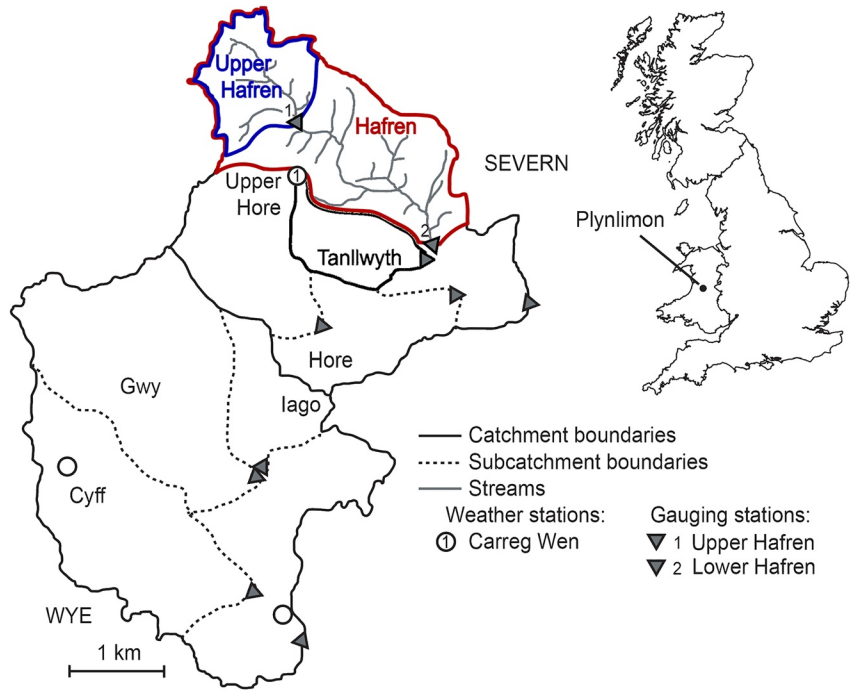

Figure 1. Plynlimon basins, Wales. We used hydrochemistry data collected weekly and at high-frequency (7 hr resolution) at the Lower and Upper Hafren gauging stations. Precipitation and its chloride concentration were simultaneously recorded at Carreg Wen station. Figure adapted from Knapp et al. (2019).

For the Lower Hafren catchment, the weekly time series includes measurements of DOC concentration in the streamflow, air temperature, chloride concentration, both in the streamflow and in the precipitation, and rainfall, the latter two sampled simultaneously at nearby Carreg Wen station. Complete observations for all variables of interest cover nearly 25 complete years, from 29 August 1984 to 31 December 2009 (1,413 total observations). Daily measures of discharge for the same period at river Hafren are provided by CEH within the National River Flow Archive (NRFA). We derived the specific daily discharge (in mm/h) knowing the total catchment area (3.58 km^2). We numerically integrated the model equation using a timestep of 6 hr, similar to the sampling interval of the high-frequency record, see below. To downscale precipitation depth and its chloride concentration from weekly to 6-hr timestep, we retrieved estimates of average catchment daily rainfall derived from gridded data (Keller et al., 2015) and distributed by the NRFA. Downscaled data are computed assuming constant precipitation intensity during the day and conserving the total chloride mass measured over the weekly interval. Discharge at 6-hr timestep was obtained by linear interpolation of daily data. For the Lower Hafren, the high-frequency record covers approximately 1 year from 6 March 2007 to 11 March 2008; however, there are several periods where streamflow DOC and chloride measurements are missing. The limited amount of data prevented us from applying the model using the high-frequency data exclusively. Nevertheless, we combined these data with the weekly ones for parameter estimation, as they can, even if for a short period, provide additional information on short-term fluctuations of solute concentrations.

Regarding the Upper Hafren catchment, the high-frequency data set is more comprehensive and allowed us to apply the model at a suitable temporal resolution using directly the above mentioned hydrochemistry variables plus discharge, which were all sampled at 7 hr intervals from 4 May 2007 to 27 January 2009 (2,174 total observations). Air temperature time series was not available for the high-frequency data set, we thus obtained it from the interpolation of the weekly data set of the Upper Hafren, which includes temperature measurements for the same period. As detailed by Neal et al. (2012) and Benettin, Kirchner, et al. (2015), the autosampler used in the high-frequency data set overflows for rainfall events larger than 1.2 mm per 7 hr. We thus corrected rainfall data and then estimated the corresponding chloride concentration using the weekly data and applying the mass balance approach described in details in Benettin, Kirchner, et al. (2015).

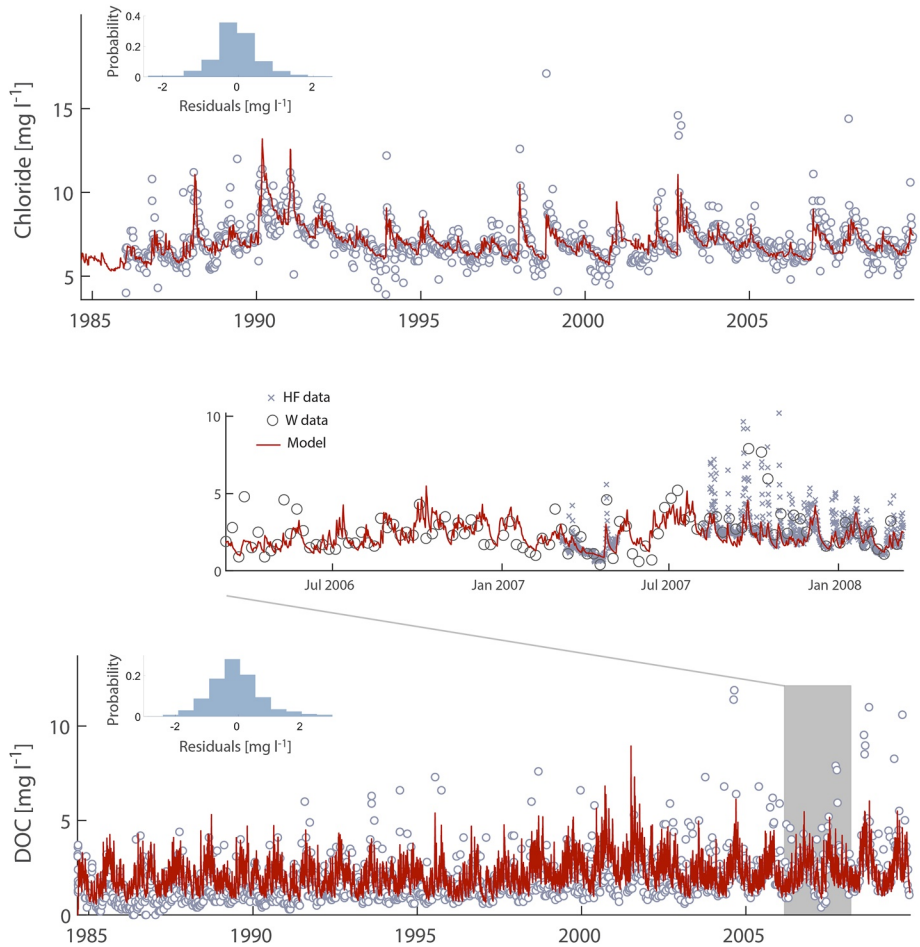

Figure 2. Chloride (upper panel) and dissolved organic carbon (DOC) (bottom panel) concentrations for the Lower Hafren series: observed data (gray circles), sampled at weekly intervals, versus model results (red solid line). For DOC, the high-frequency series sampled at 7 hr intervals from 6 March 2007 to 11 March 2008 is also displayed. The probability distributions of residuals are provided as insets. Model results shown here refer to the case where both chloride and DOC information were considered in the posterior estimation.

3.2. Model Formulations

The coupled modeling of chloride and DOC adds complexity to the scheme with respect to the typical SAS-based studies where a single tracer is accounted for. For this reason, in this first application we followed a principle of model parsimony, accounting for the most relevant processes while limiting the number of parameters. We simulated streamflow concentration of chloride and DOC via Equations 4 and Equation 8, respectively. Both variables depend on streamflow TTD p_Q, which can be computed by integrating Equation 2. The latter requires the specification of the functional form of the SAS function $\Omega_Q(S_T, t)$. van der Velde et al. (2012) initially proposed a two-parameter Beta distribution. Later Queloz et al. (2015) showed that also single-parameter power-law functions are quite flexible and can reproduce the complex behavior of reactive tracers in a lysimeter. We focused on such family of SAS functions. In particular, we used time-invariant power-law functions of the type:

$$\Omega_Q(S_T) = \left[\frac{S_T(T,t)}{S(t)}\right]^{\beta}. \tag{9}$$

For $\beta < 1$ ($\beta > 1$), the outgoing flux has a preference for younger (older) ages ($\beta = 1$ corresponds to the random sampling model where ages are sampled according to their relative abundance in the control volume). The integration of Equation 2 was performed according to the numerical scheme proposed in *tran*-SAS (Benettin & Bertuzzo, 2018) using a timestep of 6 hr for the Lower Hafren and 7 hr (the original data set frequency) for the

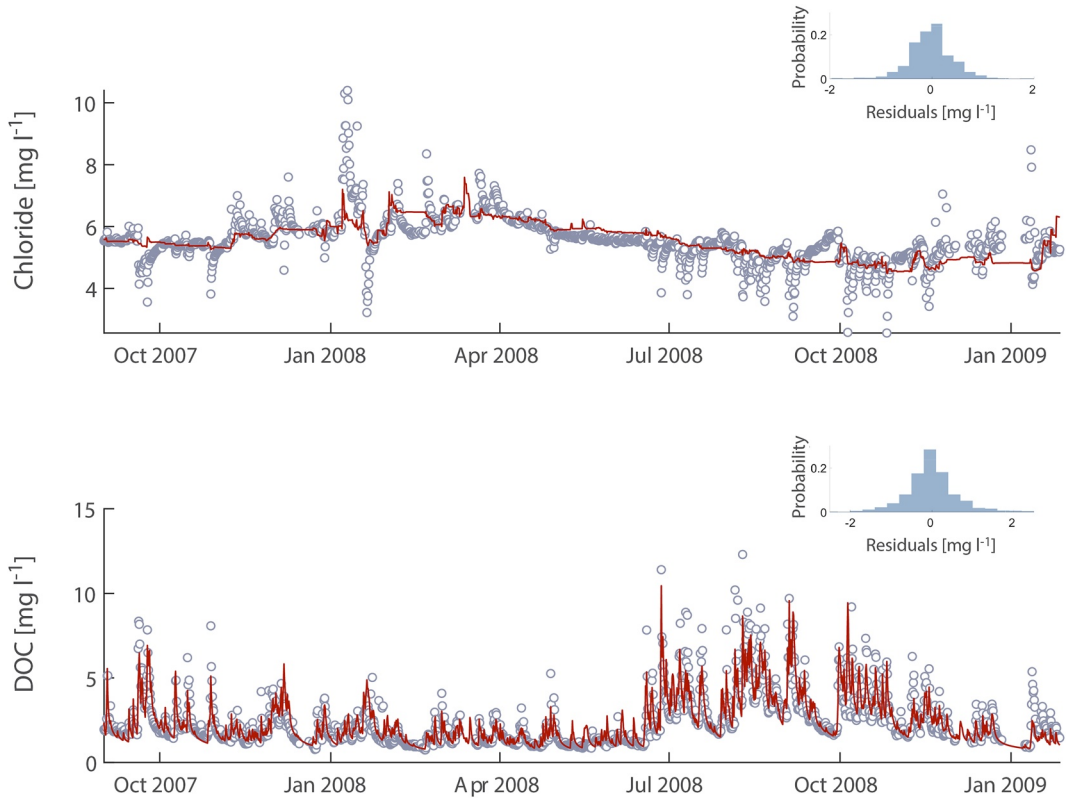

Figure 3. Chloride (upper panel) and dissolved organic carbon (DOC) (bottom panel) concentrations for the Upper Hafren high-frequency series: observed data (gray circles), sampled at 7 hr intervals, versus model simulation (red solid line). The probability distributions of residuals are also provided as insets. Model results shown here refer to the case where both chloride and DOC information were considered in the posterior estimation.

Upper Hafren. Ages up to 5 years were considered. Older water particles were pooled together in a single storage for which both the volume and the average concentration were tracked (see Benettin & Bertuzzo, 2018).

We implicitly accounted for evapotranspiration assuming that a fraction f of the precipitation eventually produces streamflow and estimated such parameter. To include the possible inputs of chloride other than precipitation (e.g., from dry or droplet deposition, Harman, 2015), we multiplied the chloride concentration in precipitation by a factor D. Accounting for both additional deposition and evapoconcentration of the rainfall input, the particularization of Equation 4 for the case at hand reads:

$$C_{\mathrm{Cl},Q}(t) = \int_0^\infty dT\, C_{\mathrm{Cl},J}(t-T)\,\frac{D}{f}\,p_Q(T,t). \tag{10}$$

We assumed that all the water already present in the system at the beginning of the simulation (volume S_0) have a chloride concentration of $C_{\mathrm{Cl,in}}$ and we estimated such parameter.

The distribution of reactivity of the initial DOC concentration, $C_{\mathrm{DOC},0}(q,t)$, is assumed to follow a gamma probability density function. This distribution has often been proposed and effectively used to model the reactivity of DOC derived from the decomposition of vegetation biomass (Aris, 1965, 1989; Bolker et al., 1998; Boudreau & Ruddick, 1991; Catalán et al., 2017, 2021; Koehler et al., 2012; Koehler & Tranvik, 2015; Tarutis, 1994). Moreover, we accounted for possible seasonality in the soil DOC concentration. Indeed, higher temperatures favor microbial activity which hence result in an increased DOC concentration. The initial concentration distribution of DOC was thus modeled as:

$$C_{\mathrm{DOC},0}(q,t) = C_{\mathrm{DOC},0}\cdot\theta^{\mathcal{T}(t)}\cdot\Gamma(q,\nu,\alpha) = C_{\mathrm{DOC},0}\,\theta^{\mathcal{T}(t)}\,\frac{\alpha^\nu}{\Gamma(\nu)}q^{\nu-1}e^{-\alpha q}. \tag{11}$$

where $\mathcal{T}(t)$ is the air temperature (in Celsius degrees) at time t, $C_{DOC,0}$ is the DOC concentration at 0 degrees Celsius, θ expresses the temperature sensitivity and $\Gamma(\cdot)$ is the gamma function. The gamma distribution is defined by two parameters: shape ν and rate α. In the following, we will refer to the the mean of the distribution $\langle q \rangle = \nu/\alpha$ rather than the rate α in order to deal with a more easily interpretable parameter.

The use of a gamma distribution for the concentration quality distribution allows for an analytical solution for the decay of the DOC concentration as age increases (Boudreau & Ruddick, 1991; Koehler et al., 2012; Koehler & Tranvik, 2015):

$$C_{DOC}(T,t) = \int_0^\infty C_{DOC}(q,T,t)dq = C_{DOC,0} \cdot \theta^{\mathcal{T}(t-T)} \left(\frac{\alpha}{\alpha+T}\right)^{\nu}. \tag{12}$$

Finally, DOC concentration in the streamflow can be obtained particularizing Equation 8 to the case at hand:

$$C_{DOC,Q}(t) = \int_0^\infty dT\, p_Q(T,t) C_{DOC}(T,t) = C_{DOC,0} \int_0^\infty dT\, p_Q(T,t) \theta^{\mathcal{T}(t-T)} \left(\frac{\alpha}{\alpha+T}\right)^{\nu}. \tag{13}$$

The average reactivity of the DOC exported via streamflow, $\langle q \rangle_Q$, can be calculated as:

$$\langle q \rangle_Q(t) = \frac{1}{C_{DOC,Q}(t)} \int_0^\infty dq\, q \int_0^\infty dT\, p_Q(T,t) C_{DOC}(q,T,t). \tag{14}$$

Although measurements or proxies of $\langle q \rangle_Q(t)$ are not available at this site, we analyzed its time series to investigate the relation between streamflow events, discharge and DOC reactivity.

3.3. Parameter Estimation

The proposed model has a total of 11 parameters (Table 1), which were estimated in a Bayesian framework. Specifically, we sampled the parameter posterior distribution using the *DREAM*$_{ZS}$ (ter Braak & Vrugt, 2008; Vrugt et al., 2009) implementation of the Markov Chain Monte Carlo algorithm. We assumed uninformative uniform prior distributions and independent, identically distributed normal errors with standard deviations equal to σ_{Cl} and σ_{DOC} for the chloride and DOC time series, respectively. We selected ranges for the uniform prior distributions (Table 1) that contain parameters typically found in the literature and broad enough to avoid any influence on the final posterior distribution (we checked that the sampled posterior had negligible values close to the prior boundaries). For both the Lower Hafren (weekly plus high-frequency) and the Upper Hafren (high-frequency only) series, we performed two different posterior samplings: in the first one only chloride data were used, while in the second one both DOC and chloride information were included in the likelihood calculation. This exercise aimed at investigating the consistency and the potential differences in the estimation of water age dynamics (namely the parameter β and S_0) when additional information (DOC data) are integrated to traditional tracer-based (chloride in this case) estimation procedures.

4. Results

We probed model performances in simultaneously reproducing DOC and chloride concentrations in the streamflow of the Lower and Upper Hafren. As regards chloride, the model is able to capture both inter-annual and intra-annual patterns exhibited in the long time-series available for Lower Hafren data set at weekly frequency (Figure 2, top panel). The resulting root mean square error (RMSE) is equal to 0.80 mg/L and the corresponding Nash-Sutcliffe efficiency (NSE) 0.50 (see Table 2 for a summary of the goodness-of-fit metrics). It should be noted, however, that some extreme values, both at the high and low ends, are not fully captured. The comparison between DOC data measured in the Lower Hafren at weekly frequency and at high frequency, when both are available (inset of Figure 2), shows how DOC has fluctuations at short time scales that are not fully captured when the process is observed at the weekly time scale. It is thus challenging for the model to reproduce this behavior when the whole data set is used for parameter estimation because high-frequency data are available only for less than 4% of the period. Nevertheless, the model captures the frequency of such fluctuations and achieves RMSE = 1.05 mg/L and NSE = 0.38. Performance in reproducing chloride concentration remained the same when only chloride data were used in the parameter estimation process (Table 2).

Table 1
List of Parameters and Posterior Statistics

Parameter	Symbol	Units	Limits	Results UH (95% C. I.)	Results LH (95% C. I.)
Exponent of the power-low SAS function	β	-	0 - 2	0.633 (0.613 - 0.655)	0.501 (0.482 - 0.521)
				0.563 (0.537 - 0.589)	0.503 (0.478 - 0.528)
Initial volume of water in storage	S_0	mm	1500 - 70000	3853 (3427 - 4320)	12637 (10953 - 14754)
				4715 (4015 - 5741)	12529 (10469 - 15728)
Effective rainfall factor	f	-	0.75 - 1	0.976 (0.921 - 0.999)	0.85 (-)
				0.859 (0.752 - 0.995)	0.85 (-)
Dry deposition factor	D	-	0.5 - 2	1.157 (1.087 - 1.200)	1.440 (1.427 - 1.453)
				0.979 (0.852 - 1.143)	1.439 (1.426 - 1.453)
Initial chloride concentration	$C_{\mathrm{Cl,in}}$	mg/l	0 - 10	7.484 (7.303 - 7.666)	5.956 (5.726 - 6.259)
				7.281 (7.082 - 7.508)	5.966 (5.650 - 6.290)
Standard deviation of Cl concentration residuals	σ_{Cl}	mg/l	0.1 - 5	0.5220 (0.504 - 0.543)	0.798 (0.770 - 0.822)
				0.518 (0.498 - 0.538)	0.798 (0.770 - 0.827)
Mean of the initial quality distribution	$\langle q \rangle$	h^{-1}	0 - 2.1	0.116 (0.010 - 0.134)	0.035 (0.028 - 0.047)
Shape of the initial quality distribution	ν	-	0 - 10	0.722 (0.688 - 0.756)	0.642 (0.584 - 0.716)
DOC concentration at 0°C	$C_{\mathrm{DOC,0}}$	mg/l	0 - 300	16.87 (15.19 - 18.70)	17.39 (15.26 - 19.90)
Temperature parameter	θ	-	1 - 1.5	1.204 (1.195 - 1.213)	1.128 (1.115 - 1.138)
Standard deviation of DOC concentration residuals	σ_{DOC}	mg/l	0.1 - 5	0.719 (0.696 - 0.744)	1.055 (1.024 - 1.088)

Note. For the Upper Hafren (UH) and Lower Hafren (LH) series, parameters resulted from the estimation processes are listed. For each parameter the median value and the 95% percentile range resulting from the sampling processes are displayed. Gray highlighted values indicate the result of the sampling strategy that uses only information about chloride. The length of the weekly time series allows a reliable estimation of the effective rainfall factor *f*. We thus estimated *f* through a mass balance between precipitation and discharge in order to avoid correlation with the parameter *D* while sampling.

The sampling frequency of DOC was not an issue for the Upper Hafren. There, the 7-hr timestep was sufficient to capture DOC concentration dynamics, which was also well reproduced by the model (Figure 3, RMSE = 0.72 mg/L, NSE = 0.79). On the other hand, performance in reproducing chloride concentration was poorer, but still comparable to that of the Lower Hafren (RMSE = 0.52 mg/L, NSE = 0.51). The model reproduces the seasonal pattern and some flow-event features, but the more pronounced fluctuations in correspondence to intense rainfall events are not captured. Similarly to the Lower Hafren, also in this case including or excluding DOC data in the parameter estimation did not lead to appreciably different results in terms of goodness-of-fit for the chloride time series (Table 2).

Figure 4 reports the sampled marginal posterior distributions for four main parameters: exponent of the power-law SAS function (β), initial volume of water in storage (S_0), mean of the initial DOC reactivity distribution ($\langle q \rangle$),

Table 2
Model Performance in Reproducing Dissolved Organic Carbon and Chloride Time Series

			RMSE (mg/L)		NSE	
Catchment	Series	Calibration	DOC	Chloride	DOC	Chloride
Lower Hafren	Weekly plus high-frequency	Chloride + DOC	1.05	0.80	0.38	0.50
Lower Hafren	Weekly plus high-frequency	Only Chloride	-	0.80	-	0.50
Upper Hafren	High frequency	Chloride + DOC	0.72	0.52	0.79	0.50
Upper Hafren	High frequency	Only Chloride	-	0.52	-	0.51

Note. Root mean square error (RMSE) and Nash-Sutcliffe efficiency coefficient (NSE) are provided for both the Upper and Lower Hafren time series of chloride and DOC in the streamflow. For both catchments, results obtained using only chloride data are also provided.

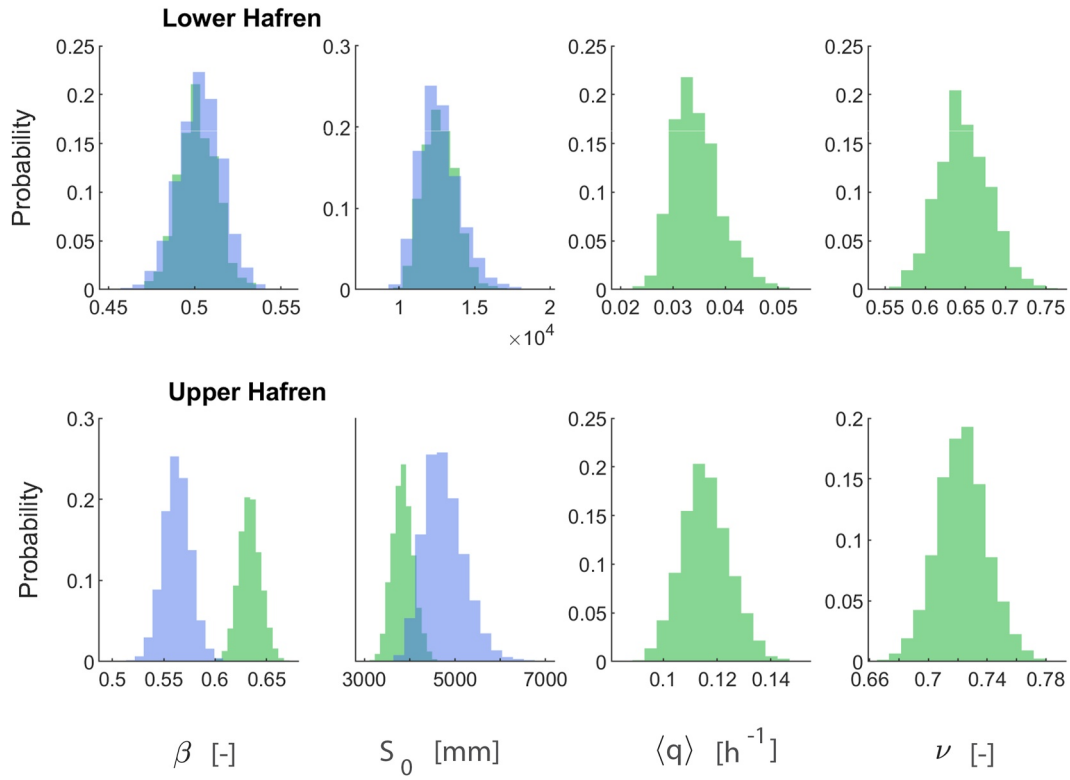

Figure 4. Posterior distributions for the four main estimated parameters (β, S_0, $\langle q \rangle$, ν) for Lower Hafren (weekly plus high-frequency time series, upper panels) and Upper Hafren (high-frequency time series, lower panels). For StorAge Selection functions parameters, results for only chloride (blue) and chloride plus dissolved organic carbon (DOC) (green) estimations are displayed, the first obtained estimating the posterior distribution using only chloride data, the latter using both chloride and DOC information.

shape of the initial reactivity distribution (ν). Information for all 11 parameters are listed in Table 1. Adding DOC data to chloride information in the estimation process reassuringly led to similar estimates for the parameters controlling the water age dynamics. Indeed, the posterior distributions in the two estimation processes show a good overlap, especially for the Lower Hafren series. Only the distributions of the parameter β in the Upper Hafren do not show an overlap, however the median values are very close (0.63 vs. 0.56). For both the Lower and Upper Hafren the β parameter was estimated to be lower than unity and around the value 0.5, which reveals a marked discharge preference to select young water. The estimated initial storage S_0 increased with the size of the catchment (median values 3,852 mm for the Upper Hafren vs. 12,637 mm for Lower Hafren). The estimated initial mean reactivity of DOC in the Upper Hafren was larger than the one estimated for the Lower Hafren (median values 0.116 hr^{-1} vs. 0.035 hr^{-1}). However, it is difficult to assess if this difference is fully attributable to different OC composition between the two catchments, or if it can partially been explained by difficulties in identifying this parameter given the issues discussed above about the low frequency of DOC sampling in the Lower Hafren. Finally, results for both catchments indicate a shape factor of the initial gamma distribution of DOC reactivity lower than unity (around 0.7), which indicates a monotonically decreasing distribution where compounds with high reactivity are progressively less abundant.

As frequently reported in the literature (see Introduction section), also this catchment presents a complex and hysteretic relation between discharge and DOC concentration. Figure 5 illustrates different examples of such hysteresis characterized by both clockwise and counterclockwise loops (i.e., DOC concentration in the rising limb of the hydrograph higher than during the falling limb for the same discharge and vivecersa, respectively) for the Upper Hafren. Notably, a rapid sequence of streamflow events can exhibit an alternation of these two distinctive behaviors (top-left panel of Figure 5a). Right panels of Figure 5a shows how the model qualitatively captures this complex hysteretic behavior for these illustrative examples. To provide a more quantitative assessment of the model performance in reproducing hysteresis loops, we calculated the hysteresis index h proposed

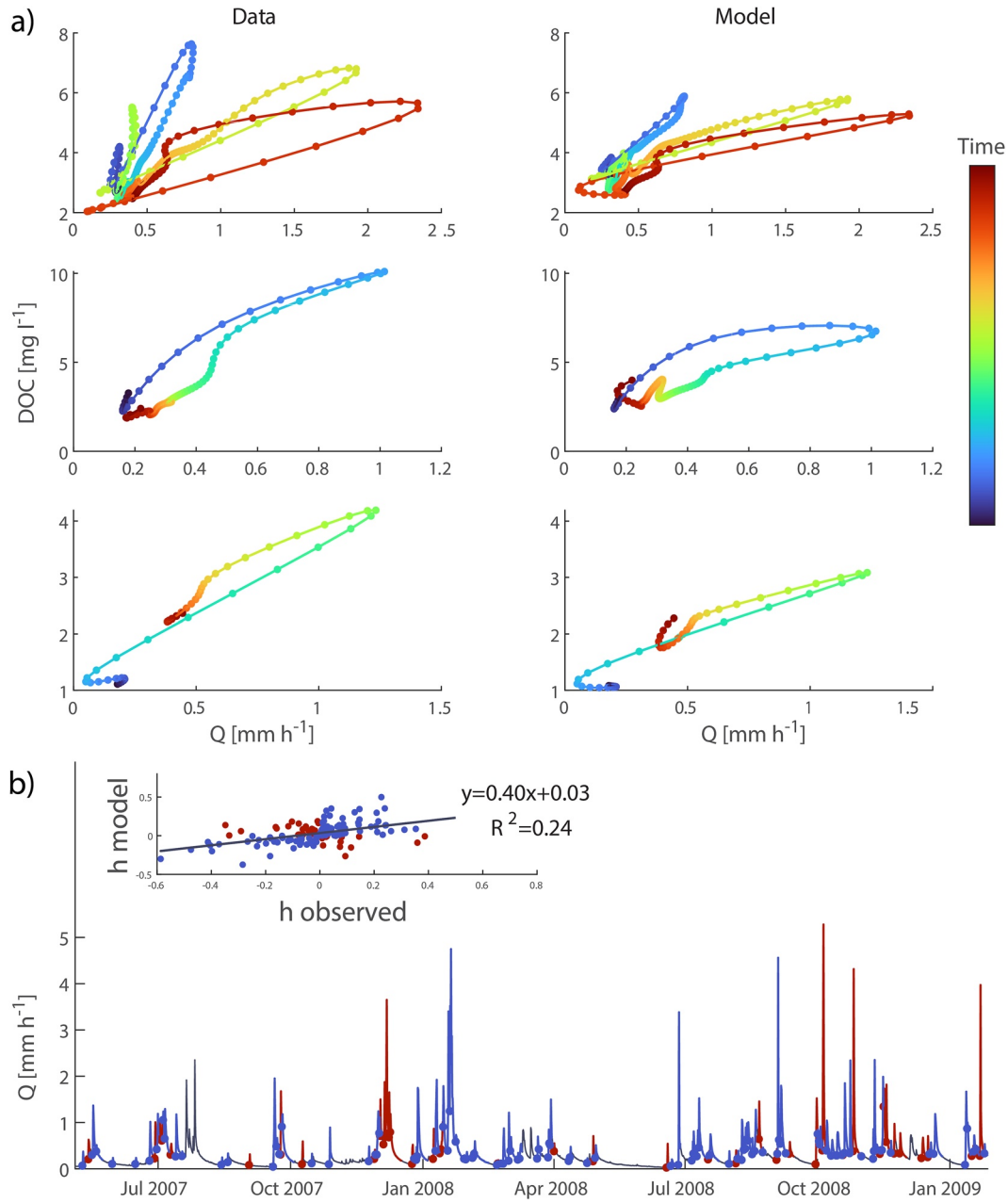

Figure 5. (a) Examples of the hysteretic discharge-dissolved organic carbon (DOC) concentration relation for the Upper Hafren time series: observed data (left panels) versus model simulation (right panels). Time series of DOC concentration and discharge (Q) were splined to 1 hr timestep to facilitate the visualization of the loops. Upper panels show different consecutive clockwise (blue, yellow) and counterclockwise (red) events from the 13th to the 25th of October 2008. Middle and bottom panels focus on two additional single clockwise and counterclockwise events, respectively, the first occurred from the 24th to 28th of June 2007 and the latter from the 28th of February to the 1st of March 2008. (b) Results for the hysteresis index h proposed by Zuecco et al. (2016) calculated from observed and modeled DOC concentration for 138 discharge events for the Upper Hafren high-frequency series. We marked the discharge time series in blue at the events which were correctly classified by the model into clockwise or counterclockwise loops and in red those that were misclassified, dots indicate the beginning of each event. The correlation between the observed and modeled values of h is also displayed in the inset with the same color code.

by Zuecco et al. (2016). Such index quantifies the hysteresis of a runoff event: it is positive for a clockwise loop and negative for a counterclockwise, and its value quantifies the area of the loop. We calculated h for 138 discharge events of different magnitude from the Upper Hafren for both the data and the model. The weekly time resolution of DOC data in the Lower Hafren precluded this analysis there. We selected events with peaks of

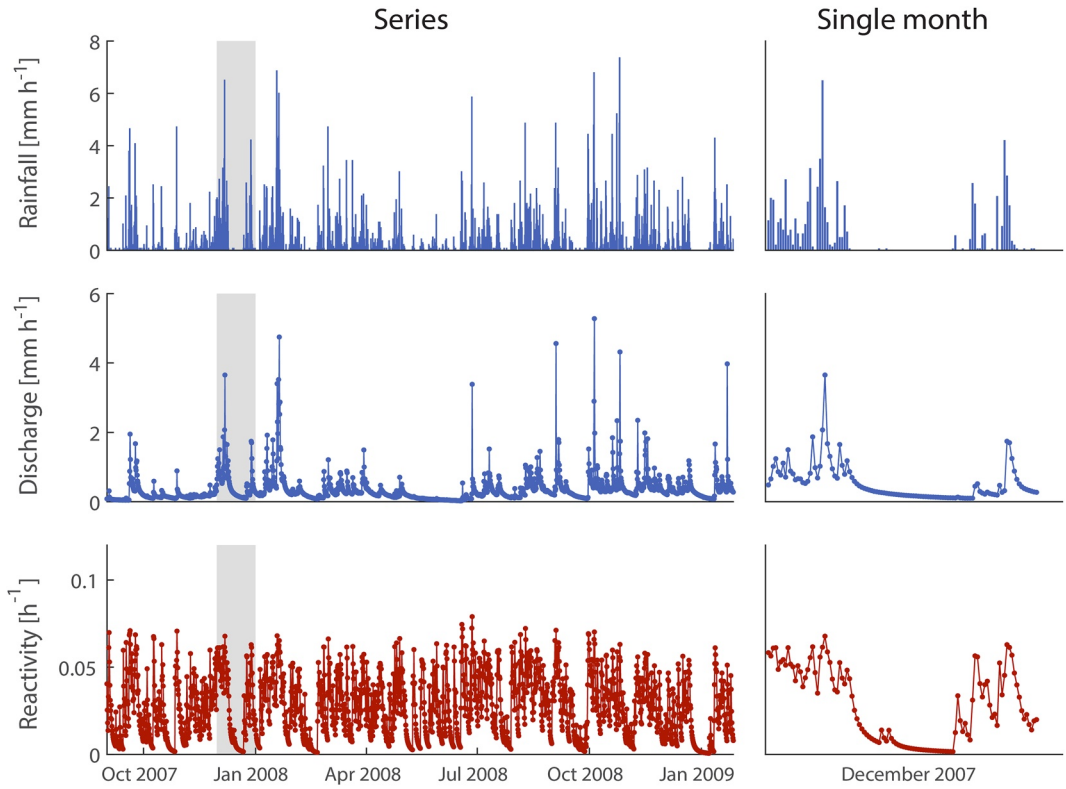

Figure 6. Simulated dissolved organic carbon reactivity in the streamflow $\langle q \rangle_Q(t)$) for the Upper Hafren (bottom panel) compared to observed rainfall and discharge series (upper and middle panels, respectively).

specific discharge greater than 1.5 mm/hr (the minimum observed flow being 0.026 mm/hr for this catchment), where data for both discharge and DOC concentration were available. The integrals of the raising and falling parts of the normalized discharge-concentration curve were computed subdividing the variability range of the normalized discharge into steps of 0.05 mm/hr and then linearly interpolating the values, as proposed by Zuecco et al. (2016). A comparison between the values of h calculated based on the observed data versus those obtained from the model results is shown in Figure 5b. The model tends to underestimate the peak concentration of DOC (see Figure 3), and this translates into an underestimation of h, as evidenced by a slope of the regression line between the two indices lower than one (inset of Figure 5b). Nevertheless, the model is able to correctly classify hysteresis events into clockwise or counterclockwise loops (i.e., the sign of h) with an accuracy of 71% (98 events correctly classified vs. 40 misclassified). The correctly classified events cover most of the time series (Figure 5b).

The proposed framework theoretically allows making predictions about the reactivity of the DOC reaching the stream. Figure 6 displays the simulated time series of average reactivity (hr^{-1}), against the observed series of rainfall and discharge for the whole Upper Hafren high-frequency data set (left panels) and for the month of December 2007 only (right panels) for illustration purpose. Reactivity appears to be very responsive to rainfall inputs showing a decrease (more recalcitrant DOC) during dry periods and a fast increase (more labile) after an event occurs.

5. Discussion

5.1. Chloride and DOC Concentrations

Results show that the proposed framework, despite its simplicity, is able to simultaneously reproduce DOC and chloride concentrations with reasonable performances. Overall, the model tends to underestimate peak concentrations, and this was particularly evident for chloride in the Upper Hafren and for DOC in the Lower Hafren. Using a similar approach for describing chloride circulation in the Lower Hafren, Harman (2015)

showed that a better performance could be achieved using a more complex model that features a two-parameter SAS-function that changes with catchment storage (NSE = 0.50 for this study vs. 0.66 for the best model obtained by Harman (2015)). Benettin, Kirchner, et al. (2015) and Rodriguez et al. (2018) showed that a more complex model formulation accounting for two compartments of soil water storage was needed to reproduce short-term fluctuations of chloride time-series in the Upper Hafren. Their performance reached a NSE of 0.69 (vs. 0.50 of our model). As introduced in the Method section, we opted here for a more parsimonious approach in view of the further complexity added by the DOC sub-model; and we therefore accepted worse performances in chloride simulation while maintaining a reasonable number of parameters. The analysis of the results and the comparison with similar applications in the literature suggest that peak concentrations of both DOC and chloride could be caused by distinctively different streamflow generation processes, like superficial or fast flow, which can only be partially reproduced with a model featuring a single storage and a time-invariant SAS function. Moreover, the comparison between the weekly and the high frequency data for the Lower Hafren (Figure 2) highlights how DOC has a very fast dynamics in this catchment, with concentration in streamflow responding quickly (with a timescale of the order of 1 day) after almost every precipitation event. Observations at weekly time scale are therefore unsuitable to monitor DOC in this site and they hamper the possibility to investigate and reproduce the underlying dynamics via a modeling exercise.

5.2. Parameters

The convergence of the posterior distributions of the SAS parameters resulting from the estimation that considers only chloride and the one which includes also information on DOC (see Figure 4) suggests that the age structure of water in the catchment inferred from tracer circulation is a good predictor also of DOC dynamics. The age of water is thus a key driver of streamflow water quality, a result supported by many other applications considering different solutes (for a review, see Hrachowitz et al., 2016). Results from both the Lower and the Upper Hafren consistently lead to an estimation of β around 0.5, confirming previous studies (Benettin, Kirchner, et al., 2015; Harman, 2015) that found a marked preference for young water in these catchments.

The estimated volume at the beginning of the simulation, S_0, for the Upper Hafren (around 3,800 mm) is close to that obtained by Benettin, Kirchner, et al. (2015) for the same catchment. The value obtained for the Lower Hafren is much larger (median value around 12,000 mm, see Figure 4 and Table 1). Although the two values refer to different dates and subcatchments, and thus they are not necessarily expected to be similar, such large difference deserves further discussion. As highlighted in Benettin, Bailey, et al. (2017), when discharge has a preference for young water, a streamwater sample conceptually comprises two components with distinctive characteristics: a young and an older water components. The former makes a large contribution to the sample and thus it controls its solute concentration. Conversely, the latter represents a mixture of all past input composition. Therefore, in the case analyzed here, the concentration of the older water component tends to the average concentration in the input for chloride and to zero for DOC (because of antecedent degradation). The total water storage, which in this formulation controls the age composition of the older water components, has thus a marginal effect on solute concentration and this frustrates its proper identification. Indeed, previous applications using similar approaches experienced similar issues. For instance, Benettin, Kirchner, et al. (2015) and Benettin, Soulsby, et al. (2017) could not properly identify an upper bound for the total storage. Hrachowitz et al. (2021) estimated a very large storage (of the order of 10,000 mm) to properly reproduce $\delta^{18}O$ time series in a headwater catchment. Finally, the model proposed by Harman (2015) for the Lower Hafren does not estimate S_0 but theoretically assumes an infinite water storage. To better understand the sensitivity of S_0 on model results, we ran an additional estimation process for the Lower Hafren using the information derived from the Upper Hafren to define a prior distribution of S_0 (Text S1 in Supporting Information S1). Starting from a prior median value of S_0 = 3,838 mm, the posterior converged to S_0 = 8,788 mm, lower than the 12,637 mm estimated with an uninformative prior (Table S1 in Supporting Information S1). The posterior distribution of all other parameters remained very similar to the case reported in the main text, except for the exponent β which was slightly higher (Table S1 in Supporting Information S1). Model performances are almost indistinguishable (see Figure S1 and Table S2 in Supporting Information S1). These results suggests that prior information on the total storage, when available, could potentially alleviate its identifiability issue, and confirm that S_0 is not critical parameter to reproduce solute dynamics when there is preference for young water. In the Text S1 in Supporting Information S1 we further compare our estimated storage and sampling function with those obtained in previous research on the Lower Hafren (Harman, 2015; Remondi et al., 2018).

The estimate of a shape factor for the gamma distribution of initial DOC reactivity ν lower than one for both the Upper and Lower Hafren aligns with previous results from experimental degradation of DOC (Catalán et al., 2017, 2021) and implies a wide spectrum of reactivity. This result also confirms the need to use the RC model to properly model DOC degradation. Indeed, the estimated distributions suggest the presence of DOC components that range from very labile to very recalcitrant, whose degradation could not be captured with a model with a single reactivity. Note that in the RC model, a single reactivity model can be well approximated by a narrow reactivity distribution which, when using a gamma distribution, could be obtained with a large shape factor.

5.3. Hysteresis

The application at high-frequency in the Upper Hafren shows that the proposed model, besides reproducing the main features of the DOC time series (Figure 3), is also able to capture, in most of the cases, its complex hysteretic behavior. The model explains this hysteresis solely by accounting for the mixing between water characterized by different age and thus DOC concentration. However, additional explanations have been proposed in the literature. For instance, a possible temporary depletion of terrestrial DOC supply due to soilwater flushing can create the more common clockwise hysteretic cycle (Raymond & Saiers, 2010). Moreover, Butturini et al. (2006) examined the concentration-discharge relations focusing on identifying the hydrological variables able to explain the variety of loops observed, and concluded that hydrology alone is not sufficient to describe the process. While we acknowledge that these other processes could be relevant, our results suggest that the time varying composition of the water age comprised in the streamflow, as modeled in the proposed framework, is a fundamental control of the discharge-DOC concentration relation. We argue that this effect is pervasive and unavoidable in most of the catchments and it should thus be properly accounted for before testing more refined hypotheses.

5.4. Limitations and Perspectives

The presented modeling framework has obvious limitations and clear avenues for improvements and further developments. We resorted to a conservatively simple scheme for TTD modeling which features a single control volume and time invariant SAS functions. This allowed us to directly use measured time-series of hydrologic fluxes (i.e., precipitation and discharge) without the need to couple a hydrologic model. Moreover, adopting power-law, invariant SAS functions allowed us to keep the free parameters to a manageable number, once those concerning the DOC modeling were also added. As discussed before, a more complex model could possibly be able to capture some features that are not well reproduced at the moment, like peak concentrations. Although these limitations do not critically impair the main objective of the study—understanding dynamics of DOC time series, at least for the case at hand, we stress the flexibility of the developed framework which can straightforwardly accommodate alternative models for the estimation of the water TTDs. Indeed, recent research on the topic has progressively developed more refined and complex models which include, for example, SAS functions that varies as a function of the catchment wetness (Harman, 2015; Nguyen et al., 2021), data-based methods to estimate TTDs (Kim & Troch, 2020) and distributed, grid-like models to account for spatial heterogeneity of TTDs (Remondi et al., 2018). In particular, we argued above how some features of the solute dynamics may not be reproduced by the model because our simple scheme cannot fully capture the behavior of contrasting streamflow generation processes. To overcome this limitation, Rodriguez and Klaus (2019) have recently proposed a composite SAS function defined as the weighted sum of different probability distributions.

Regarding carbon dynamics, we assume that DOC concentration transferred to deeper soil layers varies seasonally as a sole function of temperature, and that the concentration reaching the stream depends on the hydrologic pathway. This is tantamount to assuming that DOC export is transport limited without any supply limitation effect. Although results suggest that such simple assumption is sufficient to capture the variability of soil DOC in this application, other catchments could likely present more complex dynamics which require more realistic schemes. A first improvement that we envision is modeling a soil DOC pool that dynamically equilibrates with the soil carbon content. This simple addition could allow modeling the possible temporal depletion of DOC in the soil water after flushing precipitation events, one of the process that has been suggested to explain clockwise Q-DOC hysteretic loops (Boyer et al., 2000; Raymond & Saiers, 2010). Further improvements could explicitly consider the mass balance of soil carbon content, for which many models have already been proposed and tested in the literature, ranging from simple first-order model to complex and realistic representation of the main carbon

fluxes in soils (e.g., Jenkinson et al., 1990; Nakhavali et al., 2018; Parton et al., 1987, 1993). Mechanistic soil biogeochemical models have already been successfully combined with the TTDs approach and SAS functions to study nitrate export (Nguyen et al., 2021), and similar pathways could be followed also for DOC.

Data used herein refers to small headwater catchments and this allowed us to neglect in-stream processes and compare the DOC concentration computed for the lateral flow directly with that measured in the streamflow. Although the in-stream uptake velocity of DOC is slower than that of nutrients (Wollheim et al., 2015), in-stream processes could become relevant in large catchments (Bertuzzo et al., 2017). This calls for a network model that accounts for the responses of different subcatchments, so possibly including the spatial heterogeneity of both soil carbon dynamics and age distributions, and integrates them using a network model for in-stream processes (Bertuzzo et al., 2017). We suggest that the framework presented herein should be seen as a building block toward the development of such model.

5.5. DOC Composition and Carbon Processing in Streams

Although it was not possible to test the predicted DOC reactivity in this application, the most advanced monitoring campaigns now start to feature also high-frequency analysis of DOC quality and composition via fluorescence metrics (see e.g., Fasching et al., 2016). Therefore, we realistically foresee that in the near future these datasets could provide the opportunity for further testing and improvement of the framework proposed herein. The composition of DOC during storms has far-reaching and non trivial implications for our understanding of how river networks process and transport organic carbon drained from the terrestrial ecosystems to the coastal oceans. Indeed, the role of floods and peak flows has long been understudied because monitoring campaigns are more often carried out at base flow for practical and logistical reasons, and most large scale models work at steady state neglecting hydrologic variability. However, there is an increasing awareness that a large share of the carbon mass flux occurs during few large events (Raymond et al., 2016) because (a) OC concentration typically increases with discharge, as in this site, and (b) hydrologic conditions during high flows (high velocity and water stage) reduce the ability of the stream ecosystem to metabolize these large energy subsidies (Bertuzzo et al., 2017). The expected higher DOC reactivity during streamflow events could counterbalance the unfavorable hydrologic conditions and promote the respiration of such carbon in the stream ecosystem. Indeed, pulses of stream respiration have been reported in response to flow events (Demars, 2019). Other studies suggest that the sharp difference in quality and composition of DOC during storms can decrease the metabolic efficiency of the fluvial ecosystem because the microbial community is typically selected during baseflow conditions and thus it is adapted to process DOC with a different composition (Hitchcock & Mitrovic, 2015; Leff & Meyer, 1991; Wiegner et al., 2009). These considerations highlight the complex relation among DOC quality, hydrologic variability and the metabolic balance of river networks. As the ongoing development of sensor technology will allow an unprecedented wealth of data, it is important that also the modeling tools keep the pace in order to properly interpret this data and gain deeper insights into the dynamics of DOC in streams and rivers.

6. Conclusions

In this study we have developed a framework to estimate the export of DOC from soils to streams which combines the TTDs approach with the description of DOC degradation through the RC model. The model has been applied to two small catchments, the Lower and Upper Hafren, where data about both chloride, seen as a passive tracer useful to infer the dynamics of the age of water, and DOC concentrations were available at two different frequencies: weekly and sub-daily (7-hr timestep). The main conclusions of the study are the following:

- Despite the simplicity of the model adopted, coupling water age and RC model reproduces high-frequency DOC measurements with good performances.
- The relation between discharge and DOC concentration in the Upper Hafren shows complex hysteretic behavior, which is captured by the model solely by accounting for the mixing between water characterized by different age and thus DOC concentration.
- The comparison between the model results in the Upper and Lower Hafren shows how it is crucial to have observations of solute concentration at a frequency suitable to describe its dynamics in order to properly apply the model and gain reliable parameter estimates.

- The consistent estimation of the preference of discharge in these catchments to sample young water (parameter β) across different parameter estimation strategies (using only chloride or chloride plus DOC data), suggests that the age composition of streamflow is a key variable to predict the quantity (and potentially the reactivity) of the DOC exported from soils.
- The ability to model the reactivity of the DOC in the streamflow and how it is affected by hydrologic variability could help future studies to untangle the complex relations between carbon, water cycle and the metabolic balance of riverine ecosystems.

Finally, we discussed the presented model as a preliminary step toward the development of more realistic and large scale models that will enable us to properly interpret observed data and to shed light on the effects of hydrologic variability on how river networks, while draining water from lands to oceans, retain, respire or export organic carbon.

Data Availability Statement

Data used in this study are available online under request at the Centre of Ecology and Hydrology data catalogue. Weekly data: (https://catalogue.ceh.ac.uk/documents/44095e17-43b0-45d4-a781-aab4f72da025). High-frequency data: (https://catalogue.ceh.ac.uk/documents/551a10ae-b8ed-4ebd-ab38-033dd597a374). Daily discharge and rainfall data: (https://nrfa.ceh.ac.uk/data/station/info/54091).

Acknowledgments
The authors would like to thank two anonymous Reviewers and the Associate Editor for their insightful and constructive comments. The work was funded by the Italian Ministry of University and Research (MUR) through scholarship provided to the Doctoral School in Environmental Sciences, University of Venice Ca' Foscari.

References

Ågren, A. M., Buffam, I., Cooper, D. M., Tiwari, T., Evans, C. D., & Laudon, H. (2014). Can the heterogeneity in stream dissolved organic carbon be explained by contributing landscape elements? *Biogeosciences*, *11*(4), 1199–1213. https://doi.org/10.5194/bg-11-1199-2014

Ågren, G. I., & Bosatta, E. (1996). *Theoretical ecosystem ecology: Understanding element cycles*. Cambridge University Press.

Aris, R. (1965). Prolegomena to the rational analysis of systems of chemical reactions. *Archive for Rational Mechanics and Analysis*, *19*(2), 81–99. https://doi.org/10.1007/BF00282276

Aris, R. (1989). Reactions in continuous mixtures. *AIChE Journal*, *35*(4), 539–548. https://doi.org/10.1002/aic.690350404

Aufdenkampe, A. K., Mayorga, E., Raymond, P. A., Melack, J. M., Doney, S. C., Alin, S. R., et al. (2011). Riverine coupling of biogeochemical cycles between land, oceans, and atmosphere. *Frontiers in Ecology and the Environment*, *9*(1), 53–60. https://doi.org/10.1890/100014

Barua, S., Cartwright, I., Dresel, P. E., Morgenstern, U., McDonnell, J. J., & Daly, E. (2022). Sources and mean transit times of intermittent streamflow in semi-arid headwater catchments. *Journal of Hydrology*, *604*, 127208. https://doi.org/10.1016/j.jhydrol.2021.127208

Battin, T. J., Kaplan, L. A., Findlay, S., Hopkinson, C. S., Marti, E., Packman, A. I., et al. (2008). Biophysical controls on organic carbon fluxes in fluvial networks. *Nature Geoscience*, *1*(2), 95–100. https://doi.org/10.1038/ngeo101

Battin, T. J., Luyssaert, S., Kaplan, L., Audfenkampe, A., Richter, A., & Tranvik, L. (2009). The boundless carbon cycle. *Nature Geoscience*, *2*(9), 598–600. https://doi.org/10.1038/ngeo618

Benettin, P., Bailey, S. W., Campbell, J. L., Green, M. B., Rinaldo, A., Likens, G. E., et al. (2015). Linking water age and solute dynamics in streamflow at the Hubbard Brook Experimental Forest, NH, USA. *Water Resources Research*, *51*(11), 9256–9272. https://doi.org/10.1002/2015WR017552

Benettin, P., Bailey, S. W., Rinaldo, A., Likens, G. E., McGuire, K. J., & Botter, G. (2017). Young runoff fractions control streamwater age and solute concentration dynamics. *Hydrological Processes*, *31*(16), 2982–2986. https://doi.org/10.1002/hyp.11243

Benettin, P., & Bertuzzo, E. (2018). *tran*-SAS v1.0: A numerical model to compute catchment-scale hydrologic transport using StorAge Selection functions. *Geoscientific Model Development*, *11*(4), 1627–1639. https://doi.org/10.5194/gmd-11-1627-2018

Benettin, P., Kirchner, J., Rinaldo, A., & Botter, G. (2015). Modeling chloride transport using travel time distributions at Plynlimon, Wales. *Water Resources Research*, *51*(5), 3259–3276. https://doi.org/10.1002/2014WR016600

Benettin, P., Rinaldo, A., & Botter, G. (2015). Tracking residence times in hydrological systems: Forward and backward formulations. *Hydrological Processes*, *29*(25), 5203–5213. https://doi.org/10.1002/hyp.10513

Benettin, P., Soulsby, C., Birkel, C., Tetzlaff, D., Botter, G., & Rinaldo, A. (2017). Using SAS functions and high-resolution isotope data to unravel travel time distributions in headwater catchments. *Water Resources Research*, *53*(3), 1864–1878. https://doi.org/10.1002/2016WR020117

Bertuzzo, E., Helton, A. M., Hall, R. O., Jr., & Battin, T. J. (2017). Scaling of dissolved organic carbon removal in river networks. *Advances in Water Resources*, *110*, 136–146. https://doi.org/10.1016/j.advwatres.2017.10.009

Bertuzzo, E., Thomet, M., Botter, G., & Rinaldo, A. (2013). Catchment-scale herbicides transport: Theory and application. *Advances in Water Resources*, *52*, 232–242. https://doi.org/10.1016/j.advwatres.2012.11.007

Birkel, C., Soulsby, C., Tetzlaff, D., Dunn, S., & Spezia, L. (2012). High-frequency storm event isotope sampling reveals time-variant transit time distributions and influence of diurnal cycles. *Hydrological Processes*, *26*(2), 308–316. https://doi.org/10.1002/hyp.8210

Bolker, B. M., Pacala, S. W., & Parton, W. J., Jr. (1998). Linear analysis of soil decomposition: Insights from the century model. *Ecological Applications*, *8*(2), 425–439. https://doi.org/10.1890/1051-0761(1998)008[0425:LAOSDI]2.0.CO;2

Bosatta, E., & Ågren, G. I. (1985). Theoretical analysis of decomposition of heterogeneous substrates. *Soil Biology and Biochemistry*, *17*(5), 601–610. https://doi.org/10.1016/0038-0717(85)90035-5

Bosatta, E., & Ågren, G. I. (1991a). Dynamics of carbon and nitrogen in the organic matter of the soil: A generic theory. *The American Naturalist*, *138*(1), 227–245. https://doi.org/10.1086/285213

Bosatta, E., & Ågren, G. I. (1991b). Theoretical analysis of carbon and nutrient interactions in soils under energy-limited conditions. *Soil Science Society of America Journal*, *55*(3), 728–733. https://doi.org/10.2136/sssaj1991.03615995005500030015x

Bosatta, E., & Ågren, G. I. (1994). Theoretical analysis of microbial biomass dynamics in soils. *Soil Biology and Biochemistry*, *26*(1), 143–148. https://doi.org/10.1016/0038-0717(94)90206-2

Bosatta, E., & Ågren, G. I. (1995a). Theoretical analyses of interactions between inorganic nitrogen and soil organic matter. *European Journal of Soil Science*, *46*(1), 109–114. https://doi.org/10.1111/j.1365-2389.1995.tb01817.x

Bosatta, E., & Ågren, G. I. (1995b). The power and reactive continuum models as particular cases of the q-theory of organic matter dynamics. *Geochimica et Cosmochimica Acta*, *59*(18), 3833–3835. https://doi.org/10.1016/0016-7037(95)00287-A

Bosatta, E., & Ågren, G. I. (1996). Theoretical analyses of carbon and nutrient dynamics in soil profiles. *Soil Biology and Biochemistry*, *28*(10), 1523–1531. https://doi.org/10.1016/S0038-0717(96)00167-8

Bosatta, E., & Ågren, G. I. (2003). Exact solutions to the continuous-quality equation for soil organic matter turnover. *Journal of Theoretical Biology*, *224*(1), 97–105. https://doi.org/10.1016/S0022-5193(03)00147-4

Botter, G., Bertuzzo, E., & Rinaldo, A. (2010). Transport in the hydrologic response: Travel time distributions, soil moisture dynamics, and the old water paradox. *Water Resources Research*, *46*(3). https://doi.org/10.1029/2009WR008371

Botter, G., Bertuzzo, E., & Rinaldo, A. (2011). Catchment residence and travel time distributions: The master equation. *Geophysical Research Letters*, *38*(11). https://doi.org/10.1029/2011GL047666

Boudreau, B. P., & Ruddick, B. R. (1991). On a reactive continuum representation of organic matter diagenesis. *American Journal of Science*, *291*(5), 507–538. https://doi.org/10.2475/ajs.291.5.507

Boyer, E. W., Hornberger, G. M., Bencala, K. E., & McKnight, D. M. (1997). Response characteristics of DOC flushing in an alpine catchment. *Hydrological Processes*, *11*(12), 1635–1647. https://doi.org/10.1002/(SICI)1099-1085(19971015)11:12<1635::AID-HYP494>3.0.CO;2-H

Boyer, E. W., Hornberger, G. M., Bencala, K. E., & McKnight, D. M. (2000). Effects of asynchronous snowmelt on flushing of dissolved organic carbon: A mixing model approach. *Hydrological Processes*, *14*(18), 3291–3308. https://doi.org/10.1002/1099-1085(20001230)14:18<3291::AID-HYP202>3.0.CO;2-2

Burnham, A. K., & Braun, R. L. (1999). Global kinetic analysis of complex materials. *Energy & Fuels*, *13*(1), 1–22. https://doi.org/10.1021/ef9800765

Butturini, A., Gallart, F., Latron, J., Vazquez, E., & Sabater, F. (2006). Cross-site comparison of variability of DOC and nitrate c-q hysteresis during the autumn–winter period in three Mediterranean headwater streams: A synthetic approach. *Biogeochemistry*, *77*(3), 327–349. https://doi.org/10.1007/s10533-005-0711-7

Butturini, A., & Sabater, F. (2000). Seasonal variability of dissolved organic carbon in a Mediterranean stream. *Biogeochemistry*, *51*(3), 303–321. https://doi.org/10.1023/A:1006420229411

Carpenter, S. R. (1981). Decay of heterogenous detritus: A general model. *Journal of Theoretical Biology*, *89*(4), 539–547. https://doi.org/10.1016/0022-5193(81)90026-6

Carpenter, S. R. (1982). Comparisons of equations for decay of leaf litter in tree-hole ecosystems. *Oikos*, *39*(1), 17–22. https://doi.org/10.2307/3544526

Catalán, N., Casas-Ruiz, J., Von Schiller, D., Proia, L., Obrador, B., Zwirnmann, E., & Marcé, R. (2017). Biodegradation kinetics of dissolved organic matter chromatographic fractions in an intermittent river. *Journal of Geophysical Research: Biogeosciences*, *122*(1), 131–144. https://doi.org/10.1002/2016JG003512

Catalán, N., Obrador, B., Alomar, C., & Pretus, J. L. (2013). Seasonality and landscape factors drive dissolved organic matter properties in Mediterranean ephemeral washes. *Biogeochemistry*, *112*(1), 261–274. https://doi.org/10.1007/s10533-012-9723-2

Catalán, N., Pastor, A., Borrego, C. M., Casas-Ruiz, J. P., Hawkes, J. A., Gutiérrez, C., et al. (2021). The relevance of environment vs. composition on dissolved organic matter degradation in freshwaters. *Limnology & Oceanography*, *66*(2), 306–320. https://doi.org/10.1002/lno.11606

Clark, J., Bottrell, S., Evans, C., Monteith, D., Bartlett, R., Rose, R., et al. (2010). The importance of the relationship between scale and process in understanding long-term DOC dynamics. *Science of the Total Environment*, *408*(13), 2768–2775. https://doi.org/10.1016/j.scitotenv.2010.02.046

Cole, J., Prairie, Y., Caraco, N., McDowell, W., Tranvik, L., Striegl, R., et al. (2007). Plumbing the global carbon cycle: Integrating inland waters into the terrestrial carbon budget. *Ecosystems*, *10*(1), 172–185. https://doi.org/10.1007/s10021-006-9013-8

Cvetkovic, V., Carstens, C., Selroos, J.-O., & Destouni, G. (2012). Water and solute transport along hydrological pathways. *Water Resources Research*, *48*(6). https://doi.org/10.1029/2011WR011367

Dawson, J., Soulsby, C., Tetzlaff, D., Hrachowitz, M., Dunn, S., & Malcolm, I. (2008). Influence of hydrology and seasonality on DOC exports from three contrasting upland catchments. *Biogeochemistry*, *90*(1), 93–113. https://doi.org/10.1007/s10533-008-9234-3

Demars, B. O. (2019). Hydrological pulses and burning of dissolved organic carbon by stream respiration. *Limnology & Oceanography*, *64*(1), 406–421. https://doi.org/10.1002/lno.11048

Drake, T. W., Raymond, P. A., & Spencer, R. G. (2018). Terrestrial carbon inputs to inland waters: A current synthesis of estimates and uncertainty. *Limnology and Oceanography Letters*, *3*(3), 132–142. https://doi.org/10.1002/lol2.10055

Evans, C., Monteith, D., & Cooper, D. (2005). Long-term increases in surface water dissolved organic carbon: Observations, possible causes and environmental impacts. *Environmental pollution*, *137*, 55–71. https://doi.org/10.1016/j.envpol.2004.12.031

Fasching, C., Ulseth, A. J., Schelker, J., Steniczka, G., & Battin, T. J. (2016). Hydrology controls dissolved organic matter export and composition in an Alpine stream and its hyporheic zone. *Limnology & Oceanography*, *61*(2), 558–571. https://doi.org/10.1002/lno.10232

Haggerty, R., Wondzell, S. M., & Johnson, M. A. (2002). Power-law residence time distribution in the hyporheic zone of a 2nd-order mountain stream. *Geophysical Research Letters*, *29*(13), 1640. https://doi.org/10.1029/2002GL014743

Haria, A. H., & Shand, P. (2004). Evidence for deep sub-surface flow routing in forested upland wales: Implications for contaminant transport and stream flow generation. *Hydrology and Earth System Sciences*, *8*(3), 334–344. https://doi.org/10.5194/hess-8-334-2004

Harman, C. J. (2015). Time-variable transit time distributions and transport: Theory and application to storage-dependent transport of chloride in a watershed. *Water Resources Research*, *51*(1), 1–30. https://doi.org/10.1002/2014WR015707

Harman, C. J., & Kim, M. (2014). An efficient tracer test for time-variable transit time distributions in periodic hydrodynamic systems. *Geophysical Research Letters*, *41*(5), 1567–1575. https://doi.org/10.1002/2013GL058980

Heidbüchel, I., Troch, P. A., Lyon, S. W., & Weiler, M. (2012). The master transit time distribution of variable flow systems. *Water Resources Research*, *48*(6), W06520. https://doi.org/10.1029/2011WR011293

Hitchcock, J. N., & Mitrovic, S. M. (2015). After the flood: Changing dissolved organic carbon bioavailability and bacterial growth following inflows to estuaries. *Biogeochemistry*, *124*(1), 219–233. https://doi.org/10.1007/s10533-015-0094-3

Hornberger, G., Bencala, K., & McKnight, D. (1994). Hydrological controls on dissolved organic carbon during snowmelt in the Snake River near Montezuma, Colorado. *Biogeochemistry*, *25*(3), 147–165. https://doi.org/10.1007/BF00024390

Hrachowitz, M., Benettin, P., Van Breukelen, B. M., Fovet, O., Howden, N. J., Ruiz, L., et al. (2016). Transit times—The link between hydrology and water quality at the catchment scale. *Wiley Interdisciplinary Reviews: Water*, *3*(5), 629–657. https://doi.org/10.1002/wat2.1155

Hrachowitz, M., Savenije, H., Bogaard, T. A., Tetzlaff, D., & Soulsby, C. (2013). What can flux tracking teach us about water age distribution patterns and their temporal dynamics? *Hydrology and Earth System Sciences*, *17*(2), 533–564. https://doi.org/10.5194/hess-17-533-2013

Hrachowitz, M., Stockinger, M., Coenders-Gerrits, M., van der Ent, R., Bogena, H., Lücke, A., & Stumpp, C. (2021). Reduction of vegetation-accessible water storage capacity after deforestation affects catchment travel time distributions and increases young water fractions in a headwater catchment. *Hydrology and Earth System Sciences*, *25*(9), 4887–4915. https://doi.org/10.5194/hess-25-4887-2021

Jenkinson, D. S., Andrew, S. P. S., Lynch, J. M., Goss, M. J., Tinker, P. B., Greenwood, D. J., et al. (1990). The turnover of organic carbon and nitrogen in soil. *Philosophical Transactions of the Royal Society of London. Series B: Biological Sciences*, *329*(1255), 361–368. https://doi.org/10.1098/rstb.1990.0177

Jenkinson, D. S., & Coleman, K. (2008). The turnover of organic carbon in subsoils. Part 2. Modelling carbon turnover. *European Journal of Soil Science*, *59*(2), 400–413. https://doi.org/10.1111/j.1365-2389.2008.01026.x

Jenkinson, D. S., Poulton, P. R., & Bryant, C. (2008). The turnover of organic carbon in subsoils. Part 1. Natural and bomb radiocarbon in soil profiles from the Rothamsted long-term field experiments. *European Journal of Soil Science*, *59*(2), 391–399. https://doi.org/10.1111/j.1365-2389.2008.01025.x

Jury, W. A., Sposito, G., & White, R. E. (1986). A transfer-function model of solute transport through soil: 1. Fundamental-concepts. *Water Resources Research*, *22*(2), 243–247. https://doi.org/10.1029/WR022i002p00243

Keller, V., Tanguy, M., Prosdocimi, I., Terry, J., Hitt, O., Cole, S., et al. (2015). CEH-GEAR: 1 km resolution daily and monthly areal rainfall estimates for the UK for hydrological and other applications. *Earth System Science Data*, *7*(1), 143–155. https://doi.org/10.5194/essd-7-143-2015

Kim, M., & Troch, P. A. (2020). Transit time distributions estimation exploiting flow-weighted time: Theory and proof-of-concept. *Water Resources Research*, *56*(12), e2020WR027186. https://doi.org/10.1029/2020wr027186

Kirby, C., Newson, M., & Gilman, K. (1991). *Plynlimon research: The first two decades*. Institute of Hydrology.

Kirchner, J. W. (2009). Catchments as simple dynamical systems: Catchment characterization, rainfall-runoff modeling, and doing hydrology backward. *Water Resources Research*, *45*(2). https://doi.org/10.1029/2008WR006912

Kirchner, J. W. (2015a). Aggregation in environmental systems–Part 1: Seasonal tracer cycles quantify young water fractions, but not mean transit times, in spatially heterogeneous catchments. *Hydrology and Earth System Sciences*, *20*(1), 279–297. https://doi.org/10.5194/hess-20-279-2016

Kirchner, J. W. (2015b). Aggregation in environmental systems–Part 2: Catchment mean transit times and young water fractions under hydrologic nonstationarity. *Hydrology and Earth System Sciences*, *20*(1), 299–328. https://doi.org/10.5194/hess-20-299-2016

Kirchner, J. W., Feng, X., & Neal, C. (2000). Fractal stream chemistry and its implications for contaminant transport in catchments. *Nature*, *403*(6769), 524–527. https://doi.org/10.1038/35000537

Knapp, J. L. A., Neal, C., Schlumpf, A., Neal, M., & Kirchner, J. W. (2019). New water fractions and transit time distributions at Plynlimon, Wales, estimated from stable water isotopes in precipitation and streamflow. *Hydrology and Earth System Sciences*, *23*(10), 4367–4388. https://doi.org/10.5194/hess-23-4367-2019

Koehler, B., & Tranvik, L. J. (2015). Reactivity continuum modeling of leaf, root, and wood decomposition across biomes. *Journal of Geophysical Research: Biogeosciences*, *120*(7), 1196–1214. https://doi.org/10.1002/2015JG002908

Koehler, B., von Wachenfeldt, E., Kothawala, D., & Tranvik, L. J. (2012). Reactivity continuum of dissolved organic carbon decomposition in lake water. *Journal of Geophysical Research*, *117*(G1). https://doi.org/10.1029/2011JG001793

Kreft, A., & Zuber, A. (1978). On the physical meaning of the dispersion equation and its solutions for different initial and boundary conditions. *Chemical Engineering Science*, *33*(11), 1471–1480. https://doi.org/10.1016/0009-2509(78)85196-3

Lee, J., Whitehead, P. G., Futter, M. N., & Hall, J. W. (2020). Impacts of droughts and acidic deposition on long-term surface water dissolved organic carbon concentrations in upland catchments in Wales. *Frontiers in Environmental Science*, *8*, 193. https://doi.org/10.3389/fenvs.2020.578611

Leff, L. G., & Meyer, J. L. (1991). Biological availability of dissolved organic carbon along the Ogeechee River. *Limnology & Oceanography*, *36*(2), 315–323. https://doi.org/10.4319/lo.1991.36.2.0315

Lehmann, J., & Kleber, M. (2015). The contentious nature of soil organic matter. *Nature*, *528*(7580), 60–68. https://doi.org/10.1038/nature16069

Lyon, S. W., Mörth, M., Humborg, C., Giesler, R., & Destouni, G. (2010). The relationship between subsurface hydrology and dissolved carbon fluxes for a sub-arctic catchment. *Hydrology and Earth System Sciences*, *14*(6), 941–950. https://doi.org/10.5194/hess-14-941-2010

Maloszewski, P., Rauert, W., Trimborn, P., Herrmann, A., & Rau, R. (1992). Isotope hydrological study of mean transit times in an alpine basin (Wimbachtal, Germany). *Journal of Hydrology*, *140*(1–4), 343–360. https://doi.org/10.1016/0022-1694(92)90247-S

Manzoni, S., Katul, G. G., & Porporato, A. (2009). Analysis of soil carbon transit times and age distributions using network theories. *Journal of Geophysical Research*, *114*(G4), G04025. https://doi.org/10.1029/2009JG001070

Manzoni, S., & Porporato, A. (2009). 7 1 Soil carbon and nitrogen mineralization: Theory and models across scales. *Soil Biology and Biochemistry*, *41*(7), 1355–1379. https://doi.org/10.1016/j.soilbio.2009.02.031

Manzoni, S., Schimel, J. P., & Porporato, A. (2012). Responses of soil microbial communities to water stress: Results from a meta-analysis. *Ecology*, *93*(4), 930–938. https://doi.org/10.1890/11-0026.1

McMillan, H., Tetzlaff, D., Clark, M., & Soulsby, C. (2012). Do time-variable tracers aid the evaluation of hydrological model structure? A multimodel approach. *Water Resources Research*, *48*(5), W055010. https://doi.org/10.1029/2011WR011688

Moyano, F. E., Manzoni, S., & Chenu, C. (2013). Responses of soil heterotrophic respiration to moisture availability: An exploration of processes and models. *Soil Biology and Biochemistry*, *59*, 72–85. https://doi.org/10.1016/j.soilbio.2013.01.002

Nakhavali, M., Friedlingstein, P., Lauerwald, R., Tang, J., Chadburn, S., Camino-Serrano, M., et al. (2018). Representation of dissolved organic carbon in the JULES land surface model (vn4.4_JULES-DOCM). *Geoscientific Model Development*, *11*(2), 593–609. https://doi.org/10.5194/gmd-11-593-2018

Neal, C., & Kirchner, J. W. (2000). Sodium and chloride levels in rainfall, mist, streamwater and groundwater at the Plynlimon catchments, mid-wales: Inferences on hydrological and chemical controls. *Hydrology and Earth System Sciences*, *4*(2), 295–310. https://doi.org/10.5194/hess-4-295-2000

Neal, C., Reynolds, B., Kirchner, J. W., Rowland, P., Norris, D., Sleep, D., et al. (2013). High-frequency precipitation and stream water quality time series from Plynlimon, Wales: An openly accessible data resource spanning the periodic table. *Hydrological Processes*, *27*(17), 2531–2539. https://doi.org/10.1002/hyp.9814

Neal, C., Reynolds, B., Neal, M., Pugh, B., Hill, L., & Wickham, H. (2001). Long-term changes in the water quality of rainfall, cloud water and stream water for moorland, forested and clear-felled catchments at Plynlimon, mid-Wales. *Hydrology and Earth System Sciences*, *5*(3), 459–476. https://doi.org/10.5194/hess-5-459-2001

Neal, C., Reynolds, B., Rowland, P., Norris, D., Kirchner, J. W., Neal, M., et al. (2012). High-frequency water quality time series in precipitation and streamflow: From fragmentary signals to scientific challenge. *Science of the Total Environment*, *434*, 3–12. https://doi.org/10.1016/j.scitotenv.2011.10.072

Neal, C., Robinson, M., Reynolds, B., Neal, M., Rowland, P., Grant, S., et al. (2010). Hydrology and water quality of the headwaters of the river Severn: Stream acidity recovery and interactions with plantation forestry under an improving pollution climate. *Science of the Total Environment*, *408*(21), 5035–5051. https://doi.org/10.1016/j.scitotenv.2010.07.047

Neal, C., Robson, A., Shand, P., Edmunds, W., Dixon, A., Buckley, D., et al. (1997). The occurrence of groundwater in the Lower Palaeozoic rocks of upland Central Wales. *Hydrology and Earth System Sciences*, *1*(1), 3–18. https://doi.org/10.5194/hess-1-3-1997

Neal, C., Smith, C. J., Walls, J., Billingham, P., Hill, S., & Neal, M. (1990). Hydrogeochemical variations in Hafren forest stream waters, Mid-Wales. *Journal of Hydrology*, *116*(1), 185–200. (Transfer of Elements Through the Hydrological Cycle). https://doi.org/10.1016/0022-1694(90)90122-E

Neal, C., Wilkinson, J., Neal, M., Harrow, M., Wickham, H., Hill, L., & Morfitt, C. (1997). The hydrochemistry of the headwaters of the River Severn, Plynlimon. *Hydrology and Earth System Sciences*, *1*(3), 583–617. https://doi.org/10.5194/hess-1-583-1997

Nguyen, T. V., Kumar, R., Lutz, S. R., Musolff, A., Yang, J., & Fleckenstein, J. H. (2021). Modeling nitrate export from a mesoscale catchment using StorAge Selection functions. *Water Resources Research*, *57*(2), e2020WR028490. https://doi.org/10.1029/2020wr028490

Niemi, A. J. (1977). Residence time distributions of variable flow processes. *The International Journal of Applied Radiation and Isotopes*, *28*(10), 855–860. https://doi.org/10.1016/0020-708X(77)90026-6

Nilsson, K., Hyvönen, R., & Ågren, G. (2005). Using the continuous-quality theory to predict microbial biomass and soil organic carbon following organic amendments. *European Journal of Soil Science*, *56*(3), 397–406. https://doi.org/10.1111/j.1365-2389.2004.00677.x

Page, T., Beven, K. J., Freer, J., & Neal, C. (2007). Modelling the chloride signal at Plynlimon, Wales, using a modified dynamic TOPMODEL incorporating conservative chemical mixing (with uncertainty). *Hydrological Processes*, *21*(3), 292–307. https://doi.org/10.1002/hyp.6186

Parton, W. J., Schimel, D. S., Cole, C. V., & Ojima, D. S. (1987). Analysis of factors controlling soil organic matter levels in Great Plains grasslands. *Soil Science Society of America Journal*, *51*(5), 1173–1179. https://doi.org/10.2136/sssaj1987.03615995005100050015x

Parton, W. J., Scurlock, J. M. O., Ojima, D. S., Gilmanov, T. G., Scholes, R. J., Schimel, D. S., et al. (1993). Observations and modeling of biomass and soil organic matter dynamics for the grassland biome worldwide. *Global Biogeochemical Cycles*, *7*(4), 785–809. https://doi.org/10.1029/93GB02042

Queloz, P., Carraro, L., Benettin, P., Botter, G., Rinaldo, A., & Bertuzzo, E. (2015). Transport of fluorobenzoate tracers in a vegetated hydrologic control volume: 2. Theoretical inferences and modeling. *Water Resources Research*, *51*(4), 2793–2806. https://doi.org/10.1002/2014WR016508

Raymond, P., Hartmann, J., Lauerwald, R., Sobek, S., McDonald, C., Hoover, M., et al. (2013). Global carbon dioxide emissions from inland waters. *Nature*, *503*, 355–359. https://doi.org/10.1038/nature12760

Raymond, P., & Saiers, J. (2010). Event controlled DOC export from forested watersheds. *Biogeochemistry*, *100*(1–3), 197–209. https://doi.org/10.1007/s10533-010-9416-7

Raymond, P., Saiers, J. E., & Sobczak, W. V. (2016). Hydrological and biogeochemical controls on watershed dissolved organic matter transport: Pulse-shunt concept. *Ecology*, *97*(1), 5–16. https://doi.org/10.1890/14-1684.1

Regier, P., Briceño, H., & Jaffé, R. (2016). Long-term environmental drivers of DOC fluxes: Linkages between management, hydrology and climate in a subtropical coastal estuary. *Estuarine, Coastal and Shelf Science*, *182*, 112–122. https://doi.org/10.1016/j.ecss.2016.09.017

Remondi, F., Kirchner, J. W., Burlando, P., & Fatichi, S. (2018). Water flux tracking with a distributed hydrological model to quantify controls on the spatio-temporal variability of transit time distributions. *Water Resources Research*, *54*(4), 3081–3099. https://doi.org/10.1002/2017wr021689

Rigon, R., Bancheri, M., & Green, T. R. (2016). Age-ranked hydrological budgets and a travel time description of catchment hydrology. *Hydrology and Earth System Sciences*, *20*(12), 4929–4947. https://doi.org/10.5194/hess-20-4929-2016

Rinaldo, A., Benettin, P., Harman, C. J., Hrachowitz, M., McGuire, K. J., Van Der Velde, Y., et al. (2015). StorAge selection functions: A coherent framework for quantifying how catchments store and release water and solutes. *Water Resources Research*, *51*(6), 4840–4847. https://doi.org/10.1002/2015WR017273

Rinaldo, A., Beven, K. J., Bertuzzo, E., Nicotina, L., Davies, J., Fiori, A., et al. (2011). Catchment travel time distributions and water flow in soils. *Water Resources Research*, *47*(7). https://doi.org/10.1029/2011WR010478

Ritson, J., Graham, N., Templeton, M., Clark, J., Gough, R., & Freeman, C. (2014). The impact of climate change on the treatability of dissolved organic matter (DOM) in upland water supplies: A UK perspective. *Science of the Total Environment*, *473*, 714–730. https://doi.org/10.1016/j.scitotenv.2013.12.095

Rodriguez, N. B., & Klaus, J. (2019). Catchment travel times from composite StorAge Selection functions representing the superposition of streamflow generation processes. *Water Resources Research*, *55*(11), 9292–9314. https://doi.org/10.1029/2019WR024973

Rodriguez, N. B., McGuire, K. J., & Klaus, J. (2018). Time-varying storage–water age relationships in a catchment with a Mediterranean climate. *Water Resources Research*, *54*(6), 3988–4008. https://doi.org/10.1029/2017WR021964

Saraceno, J. F., Pellerin, B. A., Downing, B. D., Boss, E., Bachand, P. A. M., & Bergamaschi, B. A. (2009). High-frequency in situ optical measurements during a storm event: Assessing relationships between dissolved organic matter, sediment concentrations, and hydrologic processes. *Journal of Geophysical Research*, *114*(G4), G00F09. https://doi.org/10.1029/2009JG000989

Sawyer, A., Kaplan, L., Lazareva, O., & Michael, H. (2014). Hydrologic dynamics and geochemical responses within a floodplain aquifer and hyporheic zone during Hurricane Sandy. *Water Resources Research*, *50*(6), 4877–4892. https://doi.org/10.1002/2013WR015101

Soulsby, C., Birkel, C., Geris, J., Dick, J., Tunaley, C., & Tetzlaff, D. (2015). Stream water age distributions controlled by storage dynamics and nonlinear hydrologic connectivity: Modeling with high-resolution isotope data. *Water Resources Research*, *51*(9), 7759–7776. https://doi.org/10.1002/2015WR017888

Sprenger, M., Stumpp, C., Weiler, M., Aeschbach, W., Allen, S. T., Benettin, P., et al. (2019). The demographics of water: A review of water ages in the critical zone. *Reviews of Geophysics*, *57*(3), 800–834. https://doi.org/10.1029/2018RG000633

Swift, M. J., Heal, O. W., Anderson, J. M., & Anderson, J. (1979). *Decomposition in terrestrial ecosystems* (Vol. 5). University of California Press.

Tarutis, W. J. (1994). A mean-variance approach for describing organic matter decomposition. *Journal of Theoretical Biology*, *168*(1), 13–18. https://doi.org/10.1006/jtbi.1994.1083

ter Braak, C. J., & Vrugt, J. A. (2008). Differential evolution Markov chain with snooker updater and fewer chains. *Statistics and Computing*, *18*(4), 435–446. https://doi.org/10.1007/s11222-008-9104-9

Tiwari, T., Laudon, H., Beven, K., & Ågren, A. M. (2014). Downstream changes in DOC: Inferring contributions in the face of model uncertainties. *Water Resources Research*, *50*(1), 514–525. https://doi.org/10.1002/2013WR014275

Tranvik, L. J., Downing, J. A., Cotner, J. B., Loiselle, S. A., Striegl, R. G., Ballatore, T. J., et al. (2009). Lakes and reservoirs as regulators of carbon cycling and climate. *Limnology & Oceanography*, *54*(6part2), 2298–2314. https://doi.org/10.4319/lo.2009.54.6_part_2.2298

Tunaley, C., Tetzlaff, D., Lessels, J., & Soulsby, C. (2016). Linking high-frequency DOC dynamics to the age of connected water sources. *Water Resources Research*, *52*(7), 5232–5247. https://doi.org/10.1002/2015WR018419

Vähätalo, A. V., Aarnos, H., & Mäntyniemi, S. (2010). Biodegradability continuum and biodegradation kinetics of natural organic matter described by the beta distribution. *Biogeochemistry*, *100*(1), 227–240. https://doi.org/10.1007/s10533-010-9419-4

van der Velde, Y., de Rooij, G. H., Rozemeijer, J. C., van Geer, F. C., & Broers, H. P. (2010). Nitrate response of a lowland catchment: On the relation between stream concentration and travel time distribution dynamics. *Water Resources Research*, *46*(11), W11534. https://doi.org/10.1029/2010WR009105

van der Velde, Y., Heidbuchel, I., Lyon, S. W., Nyberg, L., Rodhe, A., Bishop, K., & Troch, P. A. (2014). Consequences of mixing assumptions for time-variable travel time distributions. *Hydrological Processes*, *29*(16), 3460–3474. https://doi.org/10.1002/hyp.10372

van der Velde, Y., Torfs, P. J. J. F., van der Zee, S. E. A. T. M., & Uijlenhoet, R. (2012). Quantifying catchment-scale mixing and its effect on time-varying travel time distributions. *Water Resources Research*, *48*(6). https://doi.org/10.1029/2011WR011310

Vrugt, J. A., Ter Braak, C., Diks, C., Robinson, B. A., Hyman, J. M., & Higdon, D. (2009). Accelerating Markov chain Monte Carlo simulation by differential evolution with self-adaptive randomized subspace sampling. *International Journal of Nonlinear Sciences and Numerical Stimulation*, *10*(3), 273–290. https://doi.org/10.1515/IJNSNS.2009.10.3.273

Wiegner, T. N., Tubal, R. L., & MacKenzie, R. A. (2009). Bioavailability and export of dissolved organic matter from a tropical river during base-and stormflow conditions. *Limnology & Oceanography*, *54*(4), 1233–1242. https://doi.org/10.4319/lo.2009.54.4.1233

Wollheim, W. M., Stewart, R. J., Aiken, G. R., Butler, K. D., Morse, N. B., & Salisbury, J. (2015). Removal of terrestrial DOC in aquatic ecosystems of a temperate river network. *Geophysical Research Letters*, *42*(16), 6671–6679. https://doi.org/10.1002/2015gl064647

Zuecco, G., Penna, D., Borga, M., & van Meerveld, H. J. (2016). A versatile index to characterize hysteresis between hydrological variables at the runoff event timescale. *Hydrological Processes*, *30*(9), 1449–1466. https://doi.org/10.1002/hyp.10681